



HELSINKI UNIVERSITY OF TECHNOLOGY
Faculty of Electronics, Communications and Automation
Department of Radio Science and Engineering

MARC MIR TUTUSAUS

**EVALUATION OF AUTOMOTIVE
COMMERCIAL RADAR FOR HUMAN
DETECTION**

Master of Science Thesis

Supervisor: Dr. Sampsa Koponen

Espoo, 17 – 11 – 2008

Abstract

Author: Marc Mir Tutusaus
Name of the Thesis: Evaluation of Automotive Commercial Radar for Human Detection
Date: 17 of November 2008 **Number of pages:** 75

Department: Faculty of Electronics, Communications and Automation
Department of Radio Science and Engineering
Professorship: Space Technology
Supervisor: Dr. Sampsa Koponen

Abstract:

An evaluation of the capabilities of Automotive Long Range Radar Generation 2, manufactured by Bosch, for detecting humans is presented. The main goal is to improve the security of workers in work machine environments by detecting the presence of humans and thus avoiding accidents.

In order to characterize the limitations of the radar when the target is a human instead of a car, several measurements are performed. As was expected, the measurements have shown important differences from the specifications of the radar. The maximum range has decreased from 200 m to 90 m and the angular resolution is poor. The range resolution between humans is acceptable in near range but increases when the range is large. Also, detecting a human is difficult when he is close to a larger target.

The range resolution has been identified as the main drawback in this radar. However, this radar may be able to provide better values in range resolution if the measurement configuration of the radar is changed. Different techniques for human identification have also been presented. The use of two different frequencies seems to be the most potential method to identify humans from other targets.

Keywords: Human detection, radar, sensor, automotive, work machine, FMCW, radar cross section, LRR, ACC, Bosch

Resum

La detecció de persones ha estat una activa àrea de recerca en els darrers anys i està esdevenint cada vegada més important tant en aplicacions civils com militars. Des de sistemes de vigilància fins a aplicacions de seguretat, existeix la necessitat de detectar la presència de persones autònomament per tal d'evitar intrusions en àrees restringides o per millorar-ne la seva seguretat. Detectar persones mitjançant un sensor, no obstant, és difícil per diverses raons. L'aparença d'una persona té un alt grau de variabilitat degut a la seva orientació contínuament canviant, al moviment, a les diferències de grandària i al diferent tipus de roba que porta, entre d'altres. A més, els diferents entorns on es troba la persona a detectar dificulta trobar un sensor adequat.

L'objectiu d'aquest projecte és millorar la seguretat dels treballadors en entorns de treball on maquinària pesant hi és present, detectant la seva presència i evitar així possibles danys. Aquest entorns de treball inclouen des de canteres, ports de mercaderies, mines fins altres entorns de treball on maquinària pesant hi és present. El problema en aquests entorns és que degut a la manca de visibilitat, a l'extrem soroll de fons o a les adverses condicions climàtiques és difícil veure quan una persona s'està aproximant d'una manera perillosa a una màquina. El sistema proposat constarà d'un parell de radars i altres sensors. No obstant, aquesta tesis es centra en l'anàlisi de les possibilitats i limitacions del radar. La funció principal d'aquest radar és proporcionar una certa tolerància a les difícils condicions ambientals on la majoria d'altres sensors fallen. L'abast màxim considerat adequat per a aquest sensor és d'uns 30 metres. Una altra característica important és la possibilitat de treballar en temps real, ja que un retard en la resposta pot ser crític.

La tecnologia radar s'ha aplicat amb èxit a la indústria militar durant dècades i recentment aquesta tecnologia ha estat utilitzada per la indústria de l'automòbil. La seva aplicació es pot dividir en dos camps. Per una banda, sistemes *Adaptive Cruise Control* (ACC) implementats per *Long Range Radars* (LRR) o radars de llarg abast. El sistema ACC és un sistema que proporciona informació sobre el vehicle que tenim al davant permetent accelerar, frenar i canviar de marxa automàticament. Per altre banda, aplicacions de suport a ACC, d'alerta de col·lisió, i d'ajuda a la hora d'aparcar són implementades per *Short Range Radars* (SRR) o radars de curt abast. Els LRRs

treballen a 76.5 GHz i es caracteritzen per tenir un abast d'uns 200 metres amb un camp de visió d'uns 20°. Aquests sensors utilitzen 500 MHz d'ample de banda i aconsegueixen una resolució al voltant de 0.5 metres. Per altra banda, els SRR treballen a 24 GHz i es caracteritzen per tenir un abast d'uns 30 metres amb un camp de visió d'uns 160°. Aquests sensors utilitzen 4 GHz d'ample de banda i són capaços d'aconseguir valors més alts de resolució (propers al 5 cm).

El radar escollit en aquesta tesi per analitzar les seves possibilitats reals en un sistema de detecció de persones és un *Automotive Long Range Radar 77 GHz Generation 2* produït per Bosch. La raó principal per triar un radar utilitzat a la indústria de l'automòbil és que aquesta està contínuament investigant per augmentar les possibles aplicacions del radar i reduir-ne els costos. El seu objectiu a llarg termini és l'aplicació de sensors radar no només en models de classe alta, sinó també en models de classe mitja i baixa. Tanmateix, com s'ha dit abans, hi ha dos tipus de radars utilitzats a la indústria de l'automòbil, LRR i SRR. El fet d'escollir un LRR va ser la possibilitat de disposar-ne d'un instal·lat en un automòbil per a proves a la TKK.

En el segon capítol, es proporciona informació sobre el sensor utilitzar en aquesta tesi. Per això, en primer lloc, es presenten els diferents conceptes teòrics sobre el funcionament del radar i de la modulació utilitzada. A continuació, s'exposen alguns factors que intervenen en les limitacions del radar com la difícil caracterització de la *Radar Cross Section* (RCS) d'una persona i l'elevat grau d'atenuació atmosfèrica present a altes freqüències. En el tercer capítol, es presenta una visió general de les possibles alternatives per a la detecció. Per això, es presenten els sensors d'ultrasons, làser scanners, sistemes d'infrarojos i sistemes de processament d'imatge. El capítol finalitza amb una discussió d'aquest sensors en la seva aplicació en el camp de la detecció de persones. En el quart capítol, es proporciona informació específica sobre el radar avaluat en aquesta tesi. El capítol comença presentant una visió global del LRR i a continuació cada part del radar és explicada. Es proporciona una àmplia explicació sobre la manera com el radar és capaç d'obtenir la distància i velocitat d'un objectiu. Per últim, les conseqüències en termes de degradació de la resolució en distància que té lloc al receptor són calculats per el radar utilitzat. En el cinquè capítol es presenten les mesures realitzades en aquesta tesi per tal de determinar les capacitats i limitacions del

radar quan l'objectiu a detectar és una persona. En el sisè capítol es proposen diverses tècniques més avançades d'identificació de persones mitjançant radar.

Finalment en l'últim capítol s'exposen les conclusions extretes. Els resultats d'aquest estudi conclouen que la configuració actual del LRR avaluat no és una solució adequada per al sistema proposat. La raó principal, és que el radar només és capaç de distingir una persona d'un objecte metàl·lic o d'una paret quan la distància que els separa es superior a 3 metres. Aquest fet és degut a la pobre resolució en distància que té el radar. No obstant, aquesta resolució en distància es podria incrementar, ja que el radar només utilitza 180 MHz d'ampla de banda quan és capaç d'utilitzar un ample de banda de 500 MHz. Aquest fet es deu a que l'objectiu del radar és detectar automòbils i no necessita tanta resolució en distància com la que es necessita per detectar persones. A més, el radar presenta una resolució angular quasi inexistent, propera als 12°.

El radar utilitzat només pot ser utilitzat per detectar persones i altres objectes, no per identificar quins són persones i quins no ho són. No obstant, diverses alternatives han estat estudiades. La més important és la combinació de dos radars operant a diferent freqüències. La informació proporcionada d'un objecte a dues freqüències diferents és suficient per establir un criteri per tal d'identificar persones. En futurs estudis, es podria combinar els dos radars que la indústria de l'automòbil utilitza actualment, un LRR i un SRR, ja que treballen a diferents freqüències. No obstant, enlloc d'utilitzar un LRR de segona generació, es podria utilitzar un LRR de tercera generació, amb un camp de visió més ampli i millores en resolució en distància i en resolució angular, la producció de la qual començarà a principis del 2009.

Preface

The work presented in this thesis has been carried out in the Department of Radio Science and Engineering at the Helsinki University of Technology (TKK) under the supervision of Dr. Sampsa Koponen.

Firstly, I would like to thank the supervisor of this thesis, Doctor Sampsa Koponen for introducing me to the radar field and especially for his assistance and supervision during the whole process of this work. I am grateful for the contribution of TKK and especially the Department of Radio Science and Engineering that made this work possible.

I would especially give thanks to my parents, who are great people as well as good role models, Montserrat and Josep, and to my brother, Josep Anton. My warmest thanks to my grandmothers, Maria and Montserrat, as well as to my grandfather, Antonio. Additional thanks go to my friends Josep, Teresa and Oriol.

My friends from Puigdàlber, Eloi, Ros, Michel, Roger, Lobato, Roser, Gina, Marta and Mar. Thanks to my adventure friends Aleix, Sobri, Laia, Saul and Vivi, and specially to Ruth, Roser and Faus. Finally thanks to Juliette for supporting me from a great distance.

I am also grateful to the friends who I have been sharing these last months as an exchange student facilitating me to improve my English skills. Most of all, I thank those colleges who have shared the same working space, who help me during the development of this thesis, Albert and Jaume.

Finally, I really want to thank William Martin for all the scientific writing support, for correcting and revising of all the steps during the writing process of this work.

Huge thanks go to all of you and to the ones I have not mentioned by name in this preface.

17 – 11 – 2008

Marc Mir Tutusaus

List of Terms and Abbreviations

ACC	Adaptative Cruise Control
CAN	Controller Area Network
CPU	Central Processing Unit
CW	Continuous Wave
DSP	Digital Signal Processor
ETSI	European Telecommunications Standards Institute
FFT	Fast Fourier Transform
FOV	Field of View
IEEE	Institute of Electrical and Electronics Engineers
LRR	Long Range Radar
PR	Pulsed Radar
RADAR	RAdio Detection And Ranging
RCS	Radar Cross Section
SRR	Short Range Radar

A_{ef}	effective area gain
c	speed of light
D	diameter of a circular aperture
f_b	beat frequency
f_r	beat frequency due to range
f_d	Doppler frequency
f_s	sampling frequency
f_m	modulated frequency
G	antenna gain
P_r	received power
P_t	transmitted power
R	distance between object and radar
S_i	incident power density
S_r	received power density
t_m	modulation period
v_r	radial velocity
θ_{-3dB}	-3 dB bandwidth
λ	wavelength
σ	radar cross section
τ	propagation delay
Δf	sweep frequency
Δt	sweep time

List of Tables and Figures

<i>Table 1. Standard radar frequency letter band nomenclature.</i>	16
<i>Table 2. Beamwidth as a function of the diameter of a circular aperture antenna at different frequencies calculated from Equation 2.23.</i>	24
<i>Table 3. True range versus radar range at different distances. True range is the range measured with a measuring tape, Radar range is the range measured by the radar, Error is the difference between True range and Radar range expressed in % (in respect to True range) and in meters.</i>	51
<i>Table 4. Distance where the human target is walking towards and away from the FOV can be detected.</i>	52
<i>Table 5. Distance measurements to determine the FOV using a radar reflector and a human.</i>	55
<i>Table 6. Minimum distance between human targets when they are detected as separate targets as a function of range. Radar separation is the distance between the targets measured by the radar. True separation is the distance between the targets measured with the measuring tape. Angular resolution is calculated using the radar separation. Angular error is the difference between angular resolution and the angular resolution calculated through the true separation.</i>	56
<i>Table 7. Range resolution between two humans, where human 1 and 2 are the radial distances measured by the radar, radar separation is the difference in distance between both humans measured by the radar and error is the difference between the Radar separation and the separation measured with a measuring tape.</i>	57
<i>Table 8. Distances when a human was detected as a separate target from the wall behind him for three ranges (from the radar to the wall).</i>	58
<i>Figure 1. a) FMCW triangular waveform, where the solid line represents the transmitted signal and the dashed line represent the received signal from a non-moving target. b) Beat frequency due to the FMCW waveform from Figure 1a.</i>	20
<i>Figure 2. a) Triangular FMCW waveform, where the solid line represents the transmitted signal and the dashed line represents the received signal due to a non moving target. b) Beat frequency due to the triangular FMCW waveform from figure 2a.</i>	21
<i>Figure 3. Block diagram of homodyne FMCW radar.</i>	23
<i>Figure 4. a) Moving average of the radio wave reflection intensity [5]. b) Histogram of the measured radio wave reflection intensity [5].</i>	26
<i>Figure 5. Atmospheric attenuation at millimeter waves versus frequency and wavelength at sea level and at altitude of 9150 metres in horizontal propagation [35].</i>	26
<i>Figure 6. Atmospheric attenuation due to different intensities of rainfall in millimeter waves [35].</i>	27
<i>Figure 7. The Bosch LRR evaluated in this thesis [36].</i>	38
<i>Figure 8. LRR block diagram [36].</i>	38
<i>Figure 9. System block of the microcontroler used in the signal processing unit in the radar [36].</i>	39
<i>Figure 10. Example of antenna diagram.</i>	40
<i>Figure 11. Antenna diagram of LRR2 [36].</i>	41
<i>Figure 12. FMCW signal transmitted by LRR2[36].</i>	41

Figure 13. Spectrum of an intermediate frequency[36].....	42
Figure 14. One moving target at a distance of 40 meters with 25 m/s of velocity represented solving Equation 4.1 (redrawn from [36]).	43
Figure 15.. One moving target at a distance of 40 meters with 25 m/s of velocity represented solving Equations 4.1 and 4.2 (redrawn from [36])......	44
Figure 16. Three moving targets at different distances and different velocities solving Equations 4.1, 4.2 and 4.3 (redrawn from [36]).....	44
Figure 17. Three moving targets at different distances and different velocities using an additional ramp (redrawn from [36]).....	45
Figure 18. Test vehicle with 77 GHz LRR inserted in the car insignia.....	49
Figure 19. Matlab application to present the target information on the laptop.	49
Figure 20. Football field where radar measurements is made.	50
Figure 21. Measuring method illustration for range accuracy.	51
Figure 22. Behaviour of the measurement error with distance. The blue line represents the maximum error, the red line the average error and the green line the minimum error.	52
Figure 23. Distance (Range) to a human target walking on the football field during the measurements. When the distance is above 70 m he radar loses the lock on the target.	53
Figure 24. Trihedral Reflector used to estimate the FOV.....	54
Figure 25. Measuring method illustration for FOV.....	54
Figure 26. Measuring method illustration for angular resolution and accuracy.	55
Figure 27. Measuring method illustration for range resolution between humans.....	56
Figure 28. Measuring method illustration for range resolution between human and car.	57
Figure 29. Measuring method illustration for range resolution between a row of cars and human.	58
Figure 30. From left to right: a) Measurement method illustration with a wall parallel to the FOV of the radar. b) Measurement method illustration with a wall behind the human. c) Measurement method illustration with a wall at 45 degree angle.	59
Figure 31. a) Measurement place to observe the behaviour of the radar with traffic signs. b) Measurement place to observe the behaviour of the radar with trees.	60
Figure 32. SAR measurement technique [37]......	63
Figure 33. Reflectivity of a human body with vertical and horizontal polarization in a range of 0.9-20 GHz [30]......	64
Figure 34. Receiving rates of iron and hand within a range from 10 to 60 GHz [32].	65
Figure 35. Maximum, minimum, and average values of ratio for different targets [33].	65
Figure 36. Spectrogram of a human walking obtained taking a succession of FFTs with a short time window using the output data of a CW radar at 10.525 GHz [34]......	66

Contents

Abstract	1
Resum	2
Preface	4
List of Terms and Abbreviations	6
List of Tables and Figures	7
1 Introduction.....	11
2 Radar Background	15
2.1 Radar Classification	15
2.2 Basic Radar Equation.....	16
2.3 Principles of Distance and Speed Measurements	18
2.4 Frequency Modulated Continuous Wave Principles	19
2.5 Millimeter Band Characteristics	23
2.6 Radar Cross Section.....	25
2.7 Atmospheric Attenuation	26
2.8 Conclusions.....	28
3 Alternative Sensor Technologies	29
3.1 Ultrasonic Proximity Sensor.....	29
3.2 Laser Scanner.....	31
3.3 Thermal Infrared Systems.....	32
3.4 Image Processing	34
3.5 Advantages and Disadvantage between Sensors	35
3.6 Conclusions.....	36
4 Automotive Long Range Radar 77 GHz Generation 2.....	37
4.1 Radar System	37
4.2 Antenna Beam.....	40
4.3 FMCW Signal	41
4.4 Detection Characteristics	42
4.5 Range Resolution Degradation in the Receiver	46

5	Measurements	48
5.1	Introduction.....	48
5.2	Maximum Range and Range Accuracy	50
5.3	Maximum Field of View.....	53
5.4	Angular resolution and Angular Accuracy	55
5.5	Range Resolution.....	56
5.6	Conclusions.....	60
6	Improved Radar Techniques for Human Detection and Identification.....	62
6.1	Synthetic Aperture Radar System.....	62
6.2	Polarimetric Radar	63
6.3	Dual Band Radar.....	64
6.4	Doppler Principle for Human Identification.....	66
6.5	Future Radar for Human Identification	67
7	Summary and Conclusion.....	68
	References.....	71
	Appendix.....	74
	System Parameters of the LRR2	74

Chapter 1

Introduction

Human detection has been an active research area in recent years and it is becoming increasingly important in both military and civilian applications. From surveillance systems to human security applications, there is the need to discover the presence of humans automatically in order to avoid intrusions in restricted areas or to improve the security of humans in various environments.

Detecting humans with an artificial sensor, however, is difficult for many reasons. The human appearance has a high degree of variability due to the articulated motion of a human being, orientation which is continuously changing, variable body size and the different fabrics worn by humans. Moreover, the fluctuation in the environment conditions increases the complexity of the measurement and makes it more difficult to find a suitable sensor.

In this work the word detection refers to finding the targets in the observed area. I.e., the targets are found but their type or class is not known. The word identification (or recognition) refers to the classification of targets to some useful groups (e.g., vehicles, buildings, small structures, humans and so on).

The goal of this project is to improve workers security in work machine environments by detecting the presence of humans and thus avoiding possible damages. Work machine environments include: quarries, container ports, mines and other work environments where cranes, steam shovels, big trucks and other specific machines can be present. The problem in these situations is that due to the lack of visibility, extreme background noise or adverse weather conditions it can be difficult to see a human approaching a machine in a dangerous manner.

The planned system will consist of a couple of radars and other sensors. However, this thesis is focused on analyzing the possibilities and limitations of radar sensors. The main function for the radar is to provide some tolerance to the difficult environmental conditions where most of the alternative sensors will fail. The maximum range of operation considered suitable for this sensor is around 30 meters. Another important characteristic is the possibility to work in real time, as a short response time can be critical.

Radar technologies have been successfully implemented in the military industry for decades and recently this technology has been utilized by the automotive industry. Nowadays, radar technology being used in the automotive industry is divided into two fields of applications. The first group that was introduced to the market in high class models at the beginning of the 1990's was *Adaptative Cruise Control (ACC)* performed by *Long Range Radars (LRR)*. ACC is a system to relieve the driver of the driving task maintaining a safe driving distance and warning when critical situations are near. This makes driving less strenuous, especially in flowing traffic. An ACC system provides information about traffic situations ahead of the vehicle, thus making it possible to react to altered traffic conditions by accelerating, braking or changing gear. On the other hand, ACC support, collision warning, parking aid and rear crash collision warning are performed by *Short Range Radars (SRR)*.

European Telecommunications Standard Institute (ETSI) has allocated the frequency at 76.5 GHz for LRR sensors [1]. LRRs are characterized as having a range from 1 to 200 meters with a narrow (about 20°) *Field of View (FOV)*. These sensors use 500 MHz of bandwidth achieving a range resolution of around 0.5 meters. The 24 GHz frequency has temporarily been allocated for the SRR sensors with a transition to 79 GHz in 2013 according to ETSI [2]. SRRs are characterized as having a range from 0 to 30 meters with a wide FOV (about 160°). These sensors use a 4 GHz of bandwidth achieving higher values of range resolution (approaching 5 cm).

The radar sensor chosen in this thesis to analyze the realistic possibilities in a human detection system is an Automotive Long Range Radar 77 GHz Generation 2 produced by Bosch. The main reason for choosing an automotive radar is that the automotive industry is continuously investigating radar sensors to increase the possible applications

of radar and reduce cost. The long term goal is implement radar sensors not only in high class models but also in middle and low class models. However, as stated before, there are two types of radars used by the automotive industry, LRR and SRR. Since a LRR installed in a car was available for testing at TKK, it was decided to realize this study with this radar.

Chapter 2 *Radar Background* provides information about the sensor used in this thesis. For this reason, different theoretical concepts are introduced and explained in order to lay the foundation for understanding the results and discussions of this study. The reader will be introduced to certain parts of interest within the field of basic radar theory: first of all, both the basic concepts of radar and the modulation used by the evaluated radar are introduced; then, factors involved in radar limitations are presented, and finally, advantages and disadvantages are discussed. Reading this chapter is recommended if the reader lacks prior knowledge of radar and their setup. Otherwise, Sections 2.5, 2.6, 2.7 and 2.8 contain the most important information.

Chapter 3 *Alternative Sensor Technologies* presents an overview of alternative possible sensors for object detection and a brief literature survey of ultrasonic proximity sensors, laser scanners, infrared systems and image processing is given. The chapter ends with a discussion regarding these sensors in human detection applications. If the reader is already acquainted with these sensor technologies, a brief review of Sections 3.5 and 3.6 which are specific for this work is sufficient.

Chapter 4 *Automotive Long Range Radar 77 GHz Generation 2* provides specific information about the radar evaluated in this thesis. This chapter starts by presenting a global vision of the LRR and each part of the radar is explained. An extensive explanation is given of how the radar is able to obtain distance and speed information. Finally, the consequences in terms of degradation in range resolution that take place in the receiving unit are calculated.

Chapter 5 *Measurements* shown the measurements realized in this thesis in order to determine the abilities and limitations of the radar. First, maximum and accuracy in range is fixed with humans; then, both measurements are fixed in the FOV; finally, angular and range resolution are fixed in different environments.

Chapter 6 *Improved Radar Techniques for Human Detection and Identification* proposes various more advanced radar technologies and their potential for human detection is discussed.

Chapter 7 *Summary and Conclusion* discusses the possibilities of the radar evaluated in human detection applications. A brief summary of each chapter and conclusions is presented. The chapter contains the most important contributions from the author and concludes with some recommendations regarding the direction of future research.

Chapter 2

Radar Background

This chapter provides background information about the radar sensor used in this thesis. For this reason, different theoretical concepts are introduced and explained in order to lay the foundation for understanding the results and discussions of this study. The reader will be introduced to certain parts of interest within the field of basic radar theory: first of all, both the basic concepts of radar and the modulation used by the evaluated radar are introduced; then, factors involved in radar limitations are presented, and finally, advantages and disadvantages are discussed.

2.1 Radar Classification

The word RADAR is an acronym for “*Radio Detection And Ranging*”. The operation of radar systems is based on sending radio frequency signals and measuring the signals reflected back to the radar by the objects in the propagation path of the transmitted signal (known also as backscattered signals). The signals are then processed by the radar to extract the target information such as distance, speed, angular position, as well as other target identifying characteristics.

There are numerous possible classification types of radar. In this report, however, radars are classified by the types of waveform they use and by their operating frequency. Concerning frequency classification, the range of radar frequencies has been divided into a number of bands with letter designations which are used to describe the frequency radar operation. The most common division of radar frequencies adopted by the *Institute of Electrical and Electronics Engineers (IEEE)* is shown in *Table 1* [3].

Table 1. Standard radar frequency letter band nomenclature.

Radar Letter Designation	Frequency Range	Wavelength Range
HF	3 - 30 MHz	100 - 10 m
VHF	30 - 300 MHz	10 - 1 m
UHF	300 - 1000 MHz	100 - 30 cm
L	1 - 2 GHz	30 - 15 cm
S	2 - 4 GHz	25 - 7.5 cm
C	4 - 8 GHz	7.5 - 3.75 cm
X	8 - 12 GHz	3.75 - 2.5 cm
Ku	12 - 18 GHz	2.5 - 1.67 cm
K	18 - 27 GHz	1.67 - 1.11 cm
Ka	27 - 40 GHz	1.11 - 0.75 cm
V	40 - 75 GHz	7.5 - 4.0 mm
W	75 - 110 GHz	4.0 - 2.7 mm
mm	110 - 300 GHz	2.7 - 1.0 mm

With regard to waveforms, radars can be either *Continuous Wave (CW)* or *Pulsed Radars (PR)*. CW radars are those that continuously emit electromagnetic energy. They can use both modulated and unmodulated waveforms. Modulated CW radar transmits signals in constant amplitude but modulated in frequency and can extract both distance and speed information. However, unmodulated CW radar transmits signals in constant amplitude and frequency and can only obtain speed measurements. On the other hand, PR uses a train of pulsed waveforms which can use frequency modulated or pulse modulated, in order to determine distance or speed.

2.2 Basic Radar Equation

The radar equation relates the distance of a target to the characteristics of the transmitter, receiver, antenna, target and environment. It is useful not only to determine the location of a target, but it can also serve both as a tool for understanding radar operation and as a basis for radar design. When discussing radar, the word *range* is used as a synonym for distance; similarly, the word *velocity* is used as a synonym of speed.

Considering an isotropic antenna used by radar, let P_t be the total power transmitted by the radar transmitter and R the distance between the radar and the target. An isotropic

antenna is the one which radiates uniformly in all directions. The incident power density S_i at the target is given by:

$$S_i = \frac{P_t}{4\pi R^2} \quad (2.1)$$

However, radar systems typically employ directive antennas to direct the radiated power P_t in a particular direction. The gain G of an antenna is a measure of the increased power radiated in the direction of the target as compared with the power that would have been radiated from an isotropic antenna. Thus, the incident power density S_i at the target from a directive antenna is given now by:

$$S_i = \frac{P_t G}{4\pi R^2} \quad (2.2)$$

For a single point target, the target's characteristics are accounted for through a parameter known as *Radar Cross Section* (RCS or σ), which is the measure of the amount of incident power intercepted by the target and reradiated back in the direction of the receiving radar, described in depth in Section 2.6. By the definition of RCS, the target is considered to reradiate its captured energy isotropically. Thus, the power density S_r at the radar antenna becomes:

$$S_r = \frac{P_t G}{4\pi R^2} \frac{\sigma}{4\pi R^2} \quad (2.3)$$

The signal is gained by the receiving antenna proportionally to its effective area. If the same antenna is used for both transmitting and receiving, we can apply the formula relating the effective area to the gain:

$$A_{ef} = \frac{\lambda^2}{4\pi} G \quad (2.4)$$

And rearranging the terms, finally the received power P_r becomes:

$$P_r = \frac{P_t G}{4\pi R^2} \frac{\sigma}{4\pi R^2} A_{ef} = \frac{P_t G^2 \sigma \lambda^2}{(4\pi)^3 R^4} \quad (2.5)$$

And in solving the value for a range R , the classic radar equation is obtained thus:

$$R = \sqrt[4]{\frac{P_t G^2 \sigma \lambda^2}{(4\pi)^3 P_r}} \quad (2.6)$$

Equation 2.5 gives the received power in terms of transmitted power, antenna gain, radar cross section, wavelength and the distance. However, it is a simplified version,

since neither the losses due to atmospheric attenuation nor the less than ideal features of the system are taken into account.

2.3 Principles of Distance and Speed Measurements

As stated previously, radar operates by transmitting electromagnetic energy towards the target and obtaining information concerning the location and identifying the target by detecting the backscattered energy. The distance of the target is obtained by measuring the time difference τ between the transmitted and received electromagnetic energy or, in other words, the time that a radar signal takes to travel the two way path between the radar and the target. Considering the transmitter and receiver are in the same device and the electromagnetic waves travel at the speed of light $c = 3 \times 10^8 \text{ m/s}$, the target range R can be expressed as:

$$R = \frac{c}{2} \tau \quad (2.7)$$

where R is in meters and τ is in seconds. The factor of 1/2 is needed to account for the two way time delay. For example, for a radar with a minimum detection range of 2 meters and a maximum detection range of up to 200 meters, the time difference τ to be measured is between 13.3 and 1333 ns respectively.

On the other hand, the speed of the target is obtained through the Doppler phenomenon, which describes the shift in the centre frequency of an incident waveform due to the target motion, with respect to the source radiation. Depending on the direction of the target motion this frequency shift may be either positive or negative. The Doppler frequency of target f_d can be expressed by:

$$f_d = -\frac{2}{\lambda} v_r \quad (2.8)$$

where λ is the wavelength of the radar expressed in meters and v_r is the radial velocity of the target expressed in m/s. Thus, by measuring this frequency shift, the radars can obtain directly the target radial velocity. Then, the radial velocity is given by:

$$v_r = -\frac{\lambda}{2} f_d \quad (2.9)$$

This speed will be positive if the target is moving away from the radar and will be negative if the target is moving towards the radar. For example, for a radar sensor which

operates at 76.5 GHz, Equation 2.8 gives a Doppler frequency of 510 Hz for each m/s of relative velocity. Then, if this radar can determine radial velocity between -60 to 20 m/s, the Doppler frequency will be from -30.6 KHz to 10.2 KHz.

Regarding the range accuracy and velocity accuracy there is a conflict to obtain both simultaneously. With simple wave forms such as pulsed and continuous wave radars that are not modulated in the phase, the multiplication of the standard division of errors for range and Doppler frequency is given by [4]:

$$\delta T_R \delta f = \frac{1}{\beta T_m (2S/N)} \quad (2.10)$$

where δT_R and δf are the standard division of errors for range and Doppler frequency respectively, β is the effective bandwidth of the signal, T_m is the effective time duration of the signal and S/N is the signal-to-noise ratio of the measurement.

2.4 Frequency Modulated Continuous Wave Principles

Frequency Modulated Continuous Wave (FMCW) is a range and radial velocity measuring technique. The simplest modulator scheme consists of a sawtooth wave that can only allow range measurements of a stationary target. However, in order to explain the complete method, a triangular frequency modulation is used which allow both range and velocity measurements and is close to the waveform used by the radar evaluated in the measurements as well.

In this method, the transmitter frequency is changed as a function of time in a known manner. It can be assumed that the transmitted wave is a triangular waveform as indicated by the solid line in *Figure 1a*. The transmitted waveform has constant amplitude but a frequency variation with time. If there is a reflecting object, an echo signal will return after a time τ . As can be seen, the dashed line represents the signal received from a non-moving target, being a replica of the transmitted waveform delayed.

The propagation delay τ is given by:

$$\tau = \frac{2R}{c} \quad (2.11)$$

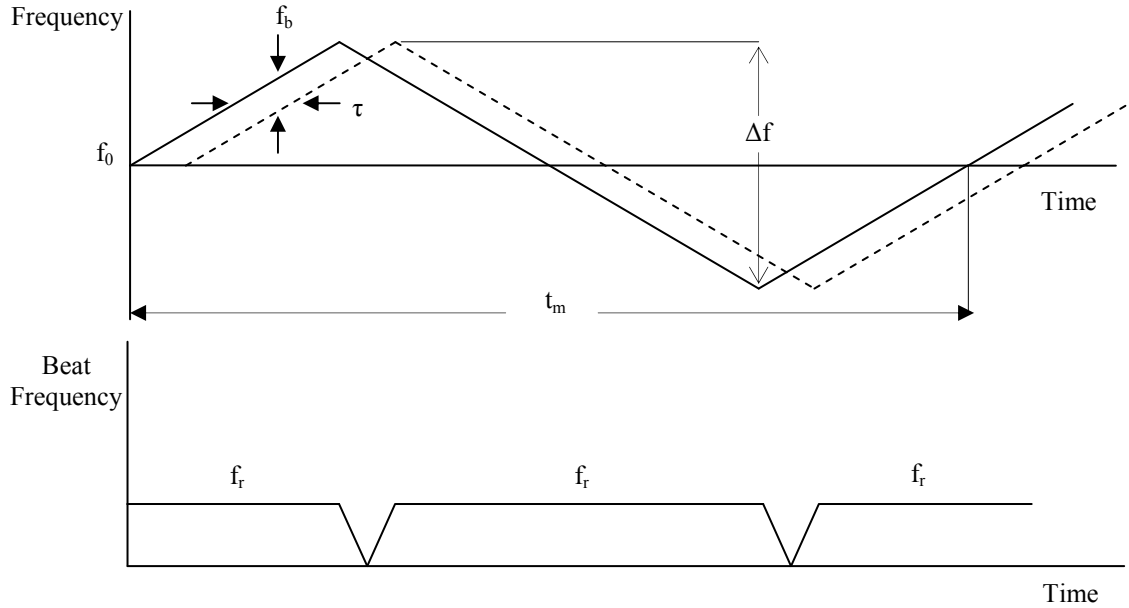


Figure 1. a) FMCW triangular waveform, where the solid line represents the transmitted signal and the dashed line represent the received signal from a non-moving target. b) Beat frequency due to the FMCW waveform from Figure 1a.

However, in contrast to other types of radar, which obtain the range measurement through the time delay, this method has to determine the frequency difference between the transmitted and received signal, known as the beat frequency (f_b) to calculate the range and velocity.

Considering a non-moving target at a distance R , the beat frequency is a measure of the target's range:

$$f_b = f_r \quad (2.12)$$

where f_r is the beat frequency resulting from the target's range. This resulting beat frequency as a function of time is shown in *Figure 1b*, in this case, the f_r directly. The beat note is a constant frequency except at the turn around region.

If the frequency is modulated at a rate f_m ($1/t_m$) over a range Δf , the beat frequency is:

$$f_b = f_r = \frac{\Delta f}{t_m/2} \tau = \frac{2\Delta f}{t_m} \frac{2R}{c} = \frac{4\Delta f R}{t_m c} \quad (2.13)$$

Rearranging the terms from *Equation 2.13*, the range is obtained as:

$$R = \frac{t_m c}{4\Delta f} f_b \quad (2.14)$$

Up to now, the target was assumed to be static. If this assumption is not applicable, the received signal will contain a Doppler frequency shift in addition to a frequency shift due to time delay τ as well.

The Doppler frequency shift causes the frequency time plot of the echo signal to be shifted either up or down, as shown in *Figure 2a*. In one portion of the frequency modulation cycle, the beat frequency is increased by the Doppler shift, while on the other portion it is decreased, as indicated by *Figure 2b*.

If, for example, the target is approaching the radar, the beat frequency f_{b+} produced during the increasing portion of the frequency modulated cycle or upsweep will be the difference between the beat frequency due to the range f_r and the Doppler frequency shift f_d , as shown in *Equation 2.15*. On the other hand, similarly, on the decreasing portion of the frequency modulated cycle or downsweep, the beat frequency f_{b-} is the sum of the two, as shown in *Equation 2.16*. These expressions are assuming that the range and velocity of the target are constant during a single modulation period. This is usually a consideration owing to the short duration of the period of the signal.

$$f_{b+} = f_r - f_d \quad (2.15)$$

$$f_{b-} = f_r + f_d \quad (2.16)$$

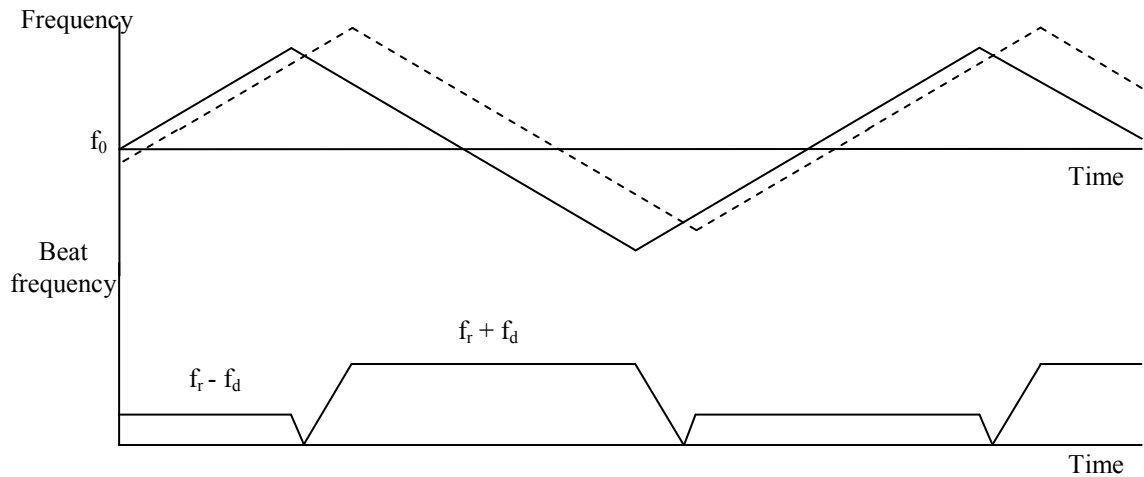


Figure 2. a) Triangular FMCW waveform, where the solid line represents the transmitted signal and the dashed line represents the received signal due to a non moving target. b) Beat frequency due to the triangular FMCW waveform from figure 2a.

The range frequency may be extracted by measuring the average beat frequency:

$$f_r = \frac{f_{b+} + f_{b-}}{2} \quad (2.17)$$

And the Doppler frequency as:

$$f_d = \frac{f_{b-} - f_{b+}}{2} \quad (2.18)$$

If the correct values of f_r and f_d have been determined, the range and radial velocity can be calculated. Since the modulation parameters t_m and Δf are known, f_r will depend on the range according to:

$$f_r = \frac{4R\Delta f}{ct_m} \quad (2.19)$$

The range can then be calculated from:

$$R = \frac{ct_m}{4\Delta f} f_r \quad (2.20)$$

and the radial velocity of the target is given by:

$$v = \frac{\lambda}{2} f_d \quad (2.21)$$

where λ is the wavelength of the radar.

When using a triangular modulation, it is commonly assumed that $|f_d| < f_r$ and the maximum allowed Doppler shift is hence bound by f_r , since *Equation 2.15* and *Equation 2.16* give incorrect results if $|f_d| > f_r$. To deal with Doppler shifts, it becomes necessary to increase Δf and/or f_m , thereby increasing the value of f_r for a given range. However, in human detection it is assumed that $|f_d| < f_r$ since the velocity of humans is small.

The accuracy of the FMCW radar is explained in detail in *Section 6.4*, since the limitation is proportional to the frequency accuracy of the receptor. In order to finalize this brief description about the FMCW radar, a block diagram illustrating the principle of the FMCW radar is shown in *Figure 3*. A *Voltage-Controlled Oscillator* (VCO) is an oscillator which varies its frequency according to the DC voltage applied. The signal produced by the VCO is at the same time transmitted through antenna and acts as the reference signal required to produce the beat frequency. Then, the beat frequency is amplified. The Fast Fourier Transform is the mathematical tool used to interpret the spectrum of the beat frequency.

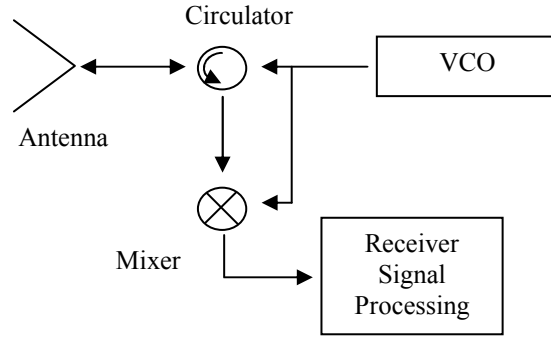


Figure 3. Block diagram of homodyne FMCW radar.

2.5 Millimeter Band Characteristics

Millimeter wave radars operate in the millimetre band which constitutes the portion of the electromagnetic spectrum with wavelengths of about one to ten millimetres (30 to 300 GHz), midway between microwave and electro-optic. Millimeter waves possess several properties which differ substantially from microwave radiation.

Shorter wavelengths allow reducing the size of the antennas. This is probably one of the most important advantages of millimeter wave systems over microwave systems. This characteristic is important in applications where size and weight are a limiting factor. Comparison of S band (7 GHz) and W band (77 GHz) frequencies shows that the antenna diameter required at the W band is less than the S band by a factor of 10.

Moreover, shorter wavelengths also involve an increase of angular resolution, since the angular resolution is directly proportional to the beamwidth. The beamwidth of the antenna is given by:

$$\theta = \frac{k\lambda}{D} \quad (2.22)$$

where θ is the half power beamwidth in radians, D is the diameter of a circular aperture, λ is the wavelength of the radar in the same units and the constant k a value between 0.9 and 1.4. A typical empirical rule of thumb equation is:

$$\theta = \frac{65\lambda}{D} \quad (2.23)$$

where θ is now in degrees.

As can be seen in *Table 2*, a circular aperture antenna with a 10 cm of diameter has a half power beamwidth of 19.5° at a frequency of 10 GHz (X band), 8.1° at a frequency of 24 GHz (K band) and 2.5° at a frequency of 77 GHz (W band in millimeter band). Hence, for a given physical antenna size, the beamwidth is smaller as the frequency increases.

The range resolution is also improved due to an extremely large bandwidth associated with millimeter waves since the range resolution of any radar is proportional to the bandwidth over which it transmits and in the millimeter range is higher than in microwave region. The high Doppler frequencies (conventionally in the audio range) provide good detection of slowly moving targets and yield more accurate Doppler measurements.

Furthermore, the ratio of wavelength to target size improves for higher frequencies, enabling better detection of small objects such as poles, wires, trees, road signs and humans. However, millimeter wave systems have significantly less range capability, due to atmospheric attenuation, which will be described in *Section 2.7*.

Although millimeter waves have been proposed for numerous applications and have been the subject of theoretical studies since the early 1950s, the technology was not unfortunately sufficiently developed during the earlier part of this period, and it was not until recent solidstate advances in the past two decades that practical devices could be developed and tested.

Table 2. Beamwidth as a function of the diameter of a circular aperture antenna at different frequencies calculated from Equation 2.23.

Antenna diameter (cm)	θ (degrees)		
	10 GHz	24 GHz	77 GHz
10	19.5	8.1	2.5
20	9.8	4.1	1.3
30	6.5	2.7	0.8

2.6 Radar Cross Section

The *Radar Cross Section* (RCS) is a parameter denoted by σ and used to characterize the scattering properties of a radar target. It represents the target's size seen by the radar or the target's ability to reflect radar signals toward the direction of the receiving antenna. The value of a radar cross section σ that is used in the radar equation is not the same as the physical area, but it is defined as an equivalent area of an isotropic sphere that will produce the same echo at the radar.

The RCS of a target is a function of the target orientation with respect to the radar, the polarisation of the incident wave, the shape of the target, the electrical properties of the target, and the frequency of operation as well. Thus, two equal targets with different positions could have different RCS values. This value is expressed in both square meters and decibels referenced to square metres (dBsm), which is equivalent a $10 \log_{10}$ (RCS in m^2).

Moreover the factors described previously involve in the RCS's value, there are other special characteristics in humans that can influence his reflective intensity. While a pedestrian is walking, his or her orientation is continuously changing; pedestrian's shapes and sizes are different; the different fabrics worn by pedestrians and the smoothness of the clothes; even the heart beat and the breathing of people can modify the reflective wave as well. Thus, one of the main inconveniences in human detection is the difficulty in characterizing the RCS values in humans due to these factors.

However, the RCS's characterization of human target has been made by Naoyuiki Yamada [5]. As can be seen in *Figure 4a*, the average value for the human's radio wave reflection intensity is about -8 dBsm. This is about 15-20 dB less than the reflection intensity of the rear of a vehicle. This study also shows that the distribution of the variance has a spread of more than 20dB, as show the *Figure 4b*.

These results are significant for this study since they were realized by a 77 GHz FMCW radar and which is the same frequency as in the radar which will be used in the measurements recorded and analyzed in this thesis.

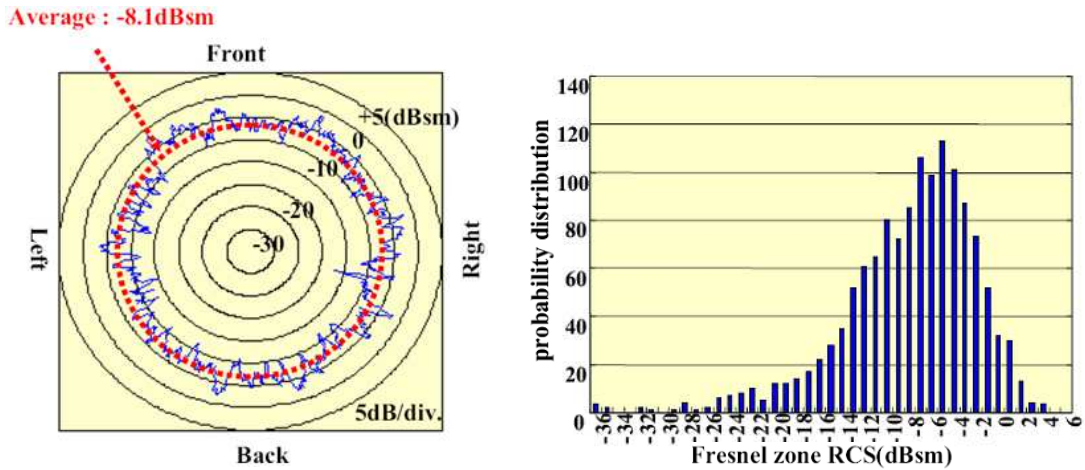


Figure 4. a) Moving average of the radio wave reflection intensity [5]. b) Histogram of the measured radio wave reflection intensity [5].

2.7 Atmospheric Attenuation

The electromagnetic energy is absorbed by atmospheric gases (water, carbon dioxide, oxygen, ozone, etc) and from attenuation due to haze, fog clouds and rain. However, each frequency presents a different absorption. The energy absorbed is converted into heat and then lost to the surrounding atmosphere. Frequency selective absorption takes place at the higher frequencies due to the resonances of the atmospheric gases and varies with atmospheric pressure, temperature and relative humidity [6].

The two most pronounced effects are due to the magnetic interaction of oxygen and the electric polarity of the water molecule in water vapour. Figure 5 shows the areas of peak absorption in the millimeter wave spectrum.

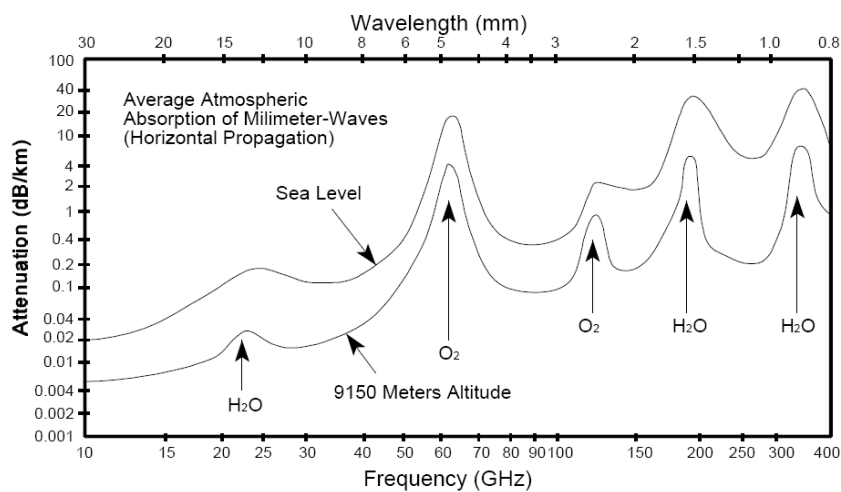


Figure 5. Atmospheric attenuation at millimeter waves versus frequency and wavelength at sea level and at altitude of 9150 metres in horizontal propagation [35].

Between the frequencies 75 and 100 GHz it can be observed that atmospheric absorption by gases is minimal. Specifically at 77 GHz, the atmospheric attenuation is 0.4 dB/km at sea level.

In order to determine the possible decrease in the signal received in adverse weather conditions, *Figure 6* shows the atmospheric attenuation resulting from the rain.

When the wavelength approaches the diameter of raindrops the drops start to act as antennas and scatter the radio waves which lead to attenuation of the signal. Fog consists of small droplets of water (the diameter of which is smaller and than the diameter of rain drops) and therefore the wavelength where its impact begins to be visible is smaller. Because of the size of the elements, fog does not cause as big attenuation at 77 GHz as does rain. The effect of snowfall depends on the water content of snowflakes, which is the reason why dry snowfall attenuates less than sleet. Additional attenuation is caused by dust and smoke.

As can be seen in the previous figure, the attenuation due to the rain at high frequencies is important, since at 77 GHz even a medium amount of rain can attenuate the signal more than 5 dB/km. Although these large values in attenuation reduce the maximum range, they contribute to interference immunity and reduce the interference between the mutual users of the band. However, neither the attenuation due to the rainfall nor the attenuation due to the atmospheric gases has any affect on the radar used in our testing, as the range is limited to 90 metres.

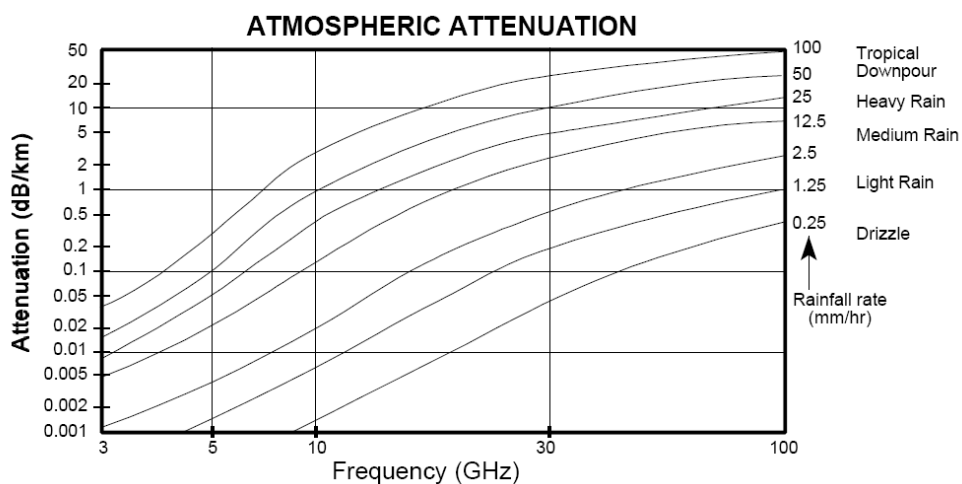


Figure 6. Atmospheric attenuation due to different intensities of rainfall in millimeter waves [35].

2.8 Conclusions

At the beginning of this chapter, the basic principles of radar and the FMCW techniques were explained. As shown, a FMCW radar is able to estimate both the distance and the velocity of the target through the measurement of the frequency changes of the received signal.

Working at millimeter wavelengths offers some advantages for the measurement. First of all, it allows the reduction of the size of the antenna and consequently the whole system. Moreover, angular resolution, Doppler and range accuracy are increased. Furthermore, millimeter wavelengths permit a decrease in the size of the detected targets. However, increases in the frequency reduce the maximum range. Atmospheric attenuation due to water vapour and oxygen is high at these frequencies although the attenuation owing to the rain is more critical.

In a human detection application, however, the main problem is the characteristics of humans. There are many factors that can modify the received signal from a human and make the human detection complicated. The radar cross section of a human is typically low and can vary considerably.

Nevertheless, considering a human detection application with a maximum range of less than 50 meters, the weather conditions do not affect the limitations of the radar. In addition, the radar sensor is able to work under both daytime and night-time operation conditions, without a high computational burden enabling work in real time.

Chapter 3

Alternative Sensor Technologies

This chapter offers a short description of all possible alternative technologies that can be used for obstacle detection, concentrating on human detection in particular. For this reason, a brief description of each alternative technology is presented, and the advantages and disadvantages in human detection are discussed. Finally, radar and these alternative sensor technologies are compared and the reasons for selecting radar for this thesis investigation are explained.

3.1 Ultrasonic Proximity Sensor

The ultrasonic proximity sensor is an example of a reflective sensor, such as a radar, that responds to changes in the amount of emitted energy returned to the detector after interaction with the target of interest.

A typical ultrasonic proximity systems consist of two transducers (one to transmit and one to receive the returned energy), although the relatively slow speed of sounds makes it possible to operate in the transceiver mode with a common transducer. The transmitter emits a longitudinal wave in the ultrasonic region of the acoustical spectrum (typically 20-200 KHz), above the normal limits of human hearing.

There are two basic types of ultrasonic proximity sensors. The first one, a pulse ultrasonic sensor, emits an ultrasonic pulse towards the target area, measuring the time interval between the pulses emitted and received to determine the presence of a target and the distance between the sensor and the target. The second one, a continuous wave ultrasonic sensor, emits a continuous ultrasonic wave towards the target area, and uses

the Doppler principle to calculate the presence of a moving target and calculate its speed.

The maximum detection range is dependent not only on the emitted power levels, but also on the target cross section, reflectivity and directivity. Ultrasonic sensors can easily obtain distance information for up to 10 meters, when the object has a large surface area, having a wide surface measurement capacity.

This solution has the advantage that it is less expensive than other sensors, due in part to the advent of low cost microcontrollers, and it is a suitable choice for both indoor and outdoor situations. Moreover, it can provide excellent accuracy and resolution in short range applications [7] and it does not require a high computational burden as other alternative systems. However, it needs to be aimed in either horizontal or vertical direction to the target, since in any other position than these two the sensor can lose the signal.

Ultrasonic proximity sensors are limited by environmental conditions that inhibit the propagation of sound waves. Such conditions include strong winds, heavy snowfall or precipitation. The nature of sound propagation limits the detector to short-range uses. In addition, ultrasonic sensors have difficulty measuring fast moving objects [8].

Another characteristic is that temperature and humidity changes can increase or decrease the size of the detection zone, since the speed of sound varies according to the temperature and pressure of the medium [9]. This is usually insignificant, but in highly sensitive applications, however, this can cause difficulties with the operation of the sensor.

Owing to the features mentioned above, applications using ultrasonic sensors can usually be found in human detection systems due to having a wide detection range angle. They are suitable in short range applications for both static and dynamic situations, as can be seen in [10]. However, another drawback of this type of sensor is that ultrasonic waves are transmitted through the air and the reflex surface texture will affect the measurement.

In [11] an ultrasonic sensor system is presented for lateral collision avoidance where it is shown that ultrasonic sensors obtain good results to detect objects in a short range of up to 6 meters with a velocity lower than 40 km/h.

3.2 Laser Scanner

Laser scanners is a sensor that measures properties of reflected light to obtain the information about targets or environments [12][13]. The laser scanner emits infrared laser pulses, typically at a wavelength from 10 micrometres up to ultraviolet light (below 400 nanometres), using a laser diode, and detects the reflected pulses.

The measurement principle is based on measuring the time delay between these pulses, where the distance to the target is directly proportional. Scanning of the measurement beam is achieved by a rotating prism and covers a viewing angle up to 360 degrees. In addition to providing a field of view of 360° in azimuth, it can also provide a wide field of view in elevation. Laser scanners can be classified as middle-long range systems due to an ability to operate up to approximately 120 metres.

Laser scanners are able to provide accurate resolution either in distance up to centimetre level and at the azimuth angle from 0.25 degree to 1 degree depending on the scanner frequency. However, the original data from the laser scanner looks like vision image data. For this reason, usually, a procedure similar to image processing is applied. First, the clustered data points are grouped into different objects by segmentation. Then the objects are classified into different categories according to their characteristics. Finally, object tracking is performed by a Kalman Filtering method [14].

Excellent range accuracy and fine angular resolution make laser scanners suitable for applications in which a high-resolution image of the surroundings is required. Moreover, operating at small wavelengths compared to radio systems such as radar, laser scanners permit detecting shorter objects than radar due to the fact in general it is possible to determine the presence of an object only about the same size as the wavelength or larger. However, since they are optical sensors, weather conditions like fog or snow will limit their detection range.

Even though it is possible to obtain excellent image quality, it takes several minutes to collect a single image due to the signal processing being a little more complex for a laser scanner compared to a microwave radar. Therefore, a dedicated CPU may be needed. There is a compromise between quality and delay since the processed data needs to be presented to the user in real time. It is necessary, therefore, to have a minimum delay between the data collection and the rendering of the imaging.

In [15], a pedestrian tracking system consisting of multiple laser scanners is proposed to track pedestrians in a wide open area. Each laser scanner is controlled by a local computer. The laser scanners are placed at the ground level and the moving feet of the pedestrians are extracted from the background. A human walking model-based Kalman filter is implemented to track the walking pedestrian. In [16], the human movement is classified by the characteristics of their moving legs.

For moving applications such as vehicles, there is the necessity to compensate for the motion. In [13] a multi laser scanner with more than one scanning plane is designed. Multiple hypothesis classification approach is used to separate the images of close targets acquired by the multilayer laser scanner in [17]. A pedestrian detection system based on a multi laser scanner is built with a field-of-view of 120 degrees in front of a vehicle in [18].

3.3 Thermal Infrared Systems

Infrared (IR) systems detect infrared radiation, electromagnetic radiation which has a wavelength between about 750 nm and 1 mm. There are several technologies using this frequency range, although this section is focused on the thermographic cameras and thermopile sensors (thermal IR).

All objects above absolute zero temperature emit infrared radiation. Thermographic camera equipment and thermopile sensors detect radiation in the infrared range and produce images with this radiation. Thus, if the features of interest are at a higher or lower temperature than the background, the thermographic camera it is able to detect them.

Imaging in the thermal infrared domain make it possible to obtain information that is not possible with the visible part of the spectrum. In the visible and near infrared, the image depends on the amount of incident light on a surface and on how well the surface reflects it. In the infrared domain, however, the image relates to the physical temperature and the emissivity of the surface.

One major point in favour of thermographic cameras and thermopiles sensors is their independence of light conditions. They can be used during both the day time or night time without any differences, extending vision beyond the usual limitations of daylight cameras. Moreover, the absence of colours or textures eases the processing requirements before interpretation.

On the other hand, however, weather conditions create difficulties by modifying the temperature of objects when there is heavy fog, snow or rain. Moreover, conditions of high temperature (e.g. summer) and the effects of direct sunlight can increase the temperature of the environment decreasing the difference of temperature between objects.

Thermographic cameras and thermopiles sensors have been used in human detection applications, since the temperature of people is higher than the temperature of the environment and their heat radiation is sufficiently high compared to the background. Obviously, other objects that actively radiate heat, such as automobiles, trucks, busses, and motorcycles, show a similar behaviour. People, fortunately, can be recognized thanks to their shape and movement [19].

In [20], a passive infrared system is suggested for near-range pedestrian detection using an array of thermopile sensors with probabilistic techniques for detection improvements. A thermopile sensor array with optimized location is designed to detect a pedestrian and estimate the pedestrian's position in [21].

The reason why thermographic cameras are used mainly in military applications is due to their high price, in contrast, thermopile sensors that have been proposed in commercial applications for human detection due to low unit costs.

3.4 Image Processing

Image processing systems are based on a camera and a microprocessor for analyzing the video image input. This type of detection is a natural choice based on the human's own experience. Although the use of a video camera make it possible to obtain objective and accurate information about the environment far richer compared to other types of sensors, this information cannot be used without being analyzed with image processing systems.

There are two main types of systems in image processing for obstacle detection: a single camera and stereo vision (two or multiple cameras). The single camera utilizes techniques like colour segmentation [22], optical flow [23] or the detection of specific characteristics in a target of interest such as texture [24] in order to determine the object of interest. The stereo-vision-based detection is a technique for directly obtaining three-dimensional depth information of objects seen by two or more video cameras from different viewpoints [24] unlike single cameras where the estimation of 3D characteristics is achieved after the detection stage.

The environmental conditions affect directly the video image quality. These conditions range from weather conditions such fog, rain, dust or snow to frost, condensation or dirt on the camera lens. Moreover, image processing is only able to operate under daylight conditions unless infrared cameras are used.

Image processing is unquestionably suited to human detection applications due to having the capacity to capture the real environment. However, the aim in image processing is to obtain correct results in real time and in uncontrolled outdoor conditions. For this reason, the development of robust and fast image processing algorithms for detection and classification is essential.

These systems can be expensive due to the cost of the cameras and the need to incorporate a device to process a heavy computation burden. However, as shown in [25], a low cost system is designed using a single optical camera with satisfactory results in the range of 0.3-20 meters.

A method for pedestrian detection is presented in [26] using two stationary cameras. The pedestrians are detected by eliminating the ground surface by transformation and matching the ground pixels in the images of both cameras.

3.5 Advantages and Disadvantage between Sensors

As stated previously, different sensors-to-object detection have been described in order to compare their advantages and disadvantages. Radar sensors, ultrasonic proximity sensors and laser scanners are all classified as active sensors, as they provide their own energy source for illuminating the target. On the other hand, thermal infrared systems and image processing are classified as passive sensors, as they measure levels of energy that are naturally emitted, reflected or transmitted by the object.

Ultrasonic proximity sensors can obtain information with high range resolution in close range objects that are less than 10 meters distance, they have a wide detection range, the cost of these sensors are less than others and using them does not require a high computational burden. However, being affected by changes in the weather conditions is a limiting factor of these sensors.

Laser scanners have a medium-to-long range with an accurate angular and range resolution and they have 360 degrees of FOV. In addition, operation is possible at smaller wavelengths than radar and ultrasonic which permit the detection of smaller objects. The downside is that the small wavelengths are attenuated more in the atmosphere especially in poor weather conditions. Further, laser scanners require a high computational burden.

Infrared systems represent the environment in terms of temperature and thus their use is not limited by light conditions. However, changes in weather conditions can modify the temperature of the objects which complicates the separation of objects from the background. Thermopile sensors are of reasonable cost when compared to thermographic cameras. Furthermore, infrared systems needs a high computational burden and cannot estimate range.

Image processing can easily obtain accurate information about the environment at a close distance. Similarly to thermal infrared systems it needs a high computational burden which make the operation difficult in real time and the equipment cost is high. In addition, environmental conditions directly affect the image quality.

3.6 Conclusions

In a human detection application there are some necessities than some of the previously mentioned sensors are not able to perform. This study maintains that a human detection system has to operate in real time with independence of weather conditions. Moreover, distance and velocity information is important to predict the movements of the human and make decisions.

Image processing and infrared systems are very promising technologies but the need for a high computational power make their use in real time situations difficult. Moreover, weather conditions affect directly in the range of coverage making the operation difficult or impossible. For these reasons image processing and thermal infrared systems are not considered as appropriate for this application.

Although ultrasonic proximity sensors are able to obtain high resolution due to their very limited range, they would not be appropriate for the application described in this project. Laser scanners are almost suitable as they have a till 360 degrees in range of coverage. Weather conditions, however, decrease the range and make this sensor unsuitable for our application.

Finally, radar is chosen instead of the before mentioned sensors due them being able to work in bad weather conditions, in real time and be able to obtain distance and range information as well.

Chapter 4

Automotive Long Range Radar 77 GHz Generation 2

The radar used in this thesis, a *Long Range Radar (LRR) 77 GHz Generation 2* produced by Bosch and used in automotive applications, in *Adaptative Cruise Control (ACC)* to be more precise, is presented and explained. The chapter starts by providing a brief description of the radar system. Then, an extensive explanation is given of how the radar is able to obtain distance and speed information. Finally, the consequences in terms of degradation in range resolution that take place in the receiving unit are calculated.

4.1 Radar System

The Bosch Automotive Long Range Radar 77 GHz Generation 2 is shown in *Figure 7*. It has considerably small dimensions, only 74x70x58 mm and the weight of the unit is less than 300 g. These characteristics allow inserting the radar in many confined places such as inside the car insignia.

A block diagram of the radar evaluated is shown below in *Figure 8*. Here, the FMCW signal is generated by a Gunn oscillator. A Gunn oscillator is an oscillator which uses a Gunn diode to produce low power signals in high frequency ranges. These oscillators are produced using *Gallium Arsenide (GaAs)* chip technology, however, *Silicon Germanium (SiGe)* has been indentified as the chip technology which may fulfil the technological requirements and reduce the cost in the next generations of LRR [27].



Figure 7. The Bosch LRR evaluated in this thesis [36].

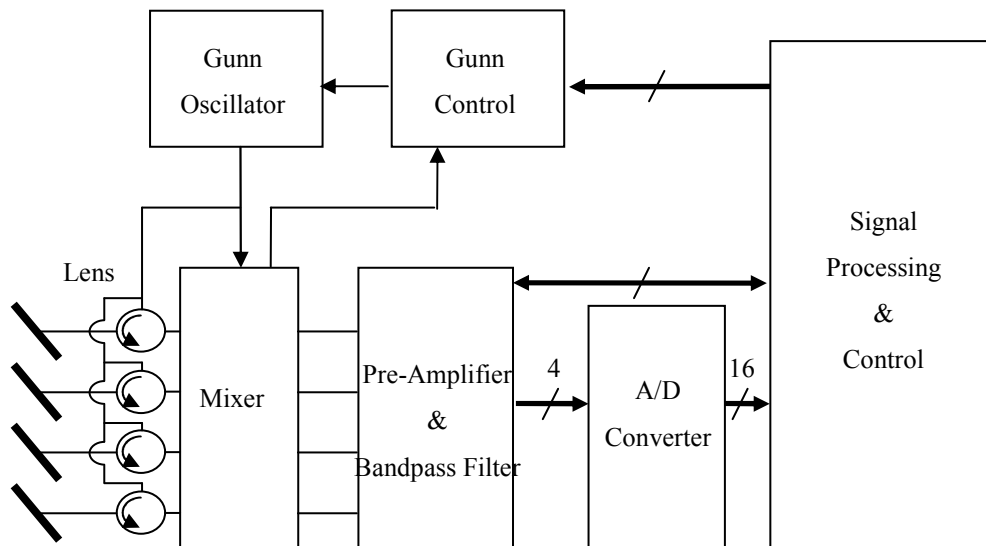


Figure 8. LRR block diagram [36].

The signal generated by the Gunn oscillator at frequency f_t is routed directly to the mixer and to each antenna through a circulator. Using a circulator the antenna is able to transmit and receive at the same time.

The received signals now have a frequency of $f_t + \Delta f$ and are homodyned (mixed) with the current transmitted signal at frequency f_t in the mixer to produce the beat

signals at frequency f_b . These beat signals now have a lower frequency than the transmitted signal. This signal is then amplified with a low noise pre-amplifier and filtered by a band pass filter to eliminate the beat frequency due to the signal transmitted and to limit the bandwidth of the signal. Then, this signal is digitalized by a four channel *Analog-Digital Converter* (ADC) at a sampling rate f_s .

The collection of samples is then passed through *Fast Fourier Transform* (FFT) algorithms, which is used to provide fast data analysis. These algorithms are performed using a microcontroller TMS470R1VF76B where his system block is shown in *Figure 9*. This microcontroller contain a *Digital Signal Processing* (DSP) working at 60 MHz and a *Central Processing Unit* (CPU) working at 40 MHz to perform control tasks.

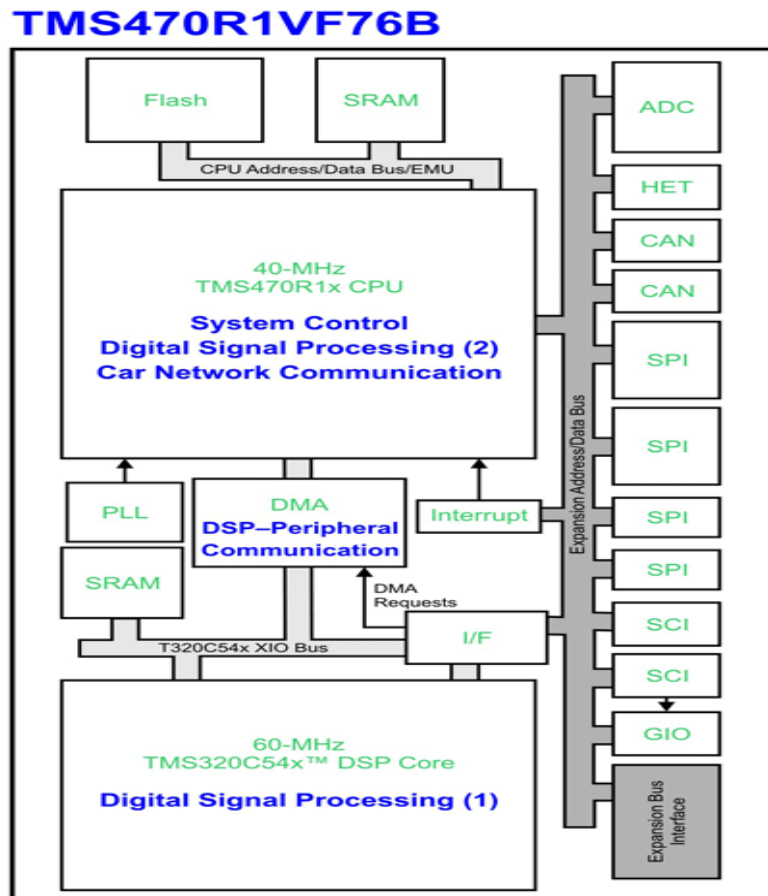


Figure 9. System block of the microcontroller used in the signal processing unit in the radar [36].

4.2 Antenna Beam

The basic function of the radar antenna is to transmit the radio frequency energy generated by the radar into the propagation medium, in this case the air, and receive the energy backscattered from the objects. In addition, the antenna concentrates the radiated power into a desired direction and provides with gain this direction in both transmission and reception as in this case the antenna is used for both transmission and reception.

As can be seen in *Figure 10*, the direction of the maximum is known as the main lobe whereas the other lobes are known as side lobes. The side lobes are the main source of interferences. One of the most important parameters is the angular width of the main lobe as it is a useful measure to determine the capability of the radar for resolving angular position. Particularly, the angle between the two points of one lobe where the power has fallen to half or 3 dB is known as the -3 dB bandwidth or θ_{-3dB} .

If several receiving antennas are used, there is the possibility to obtain angular position determining the exact angle of a target by applying comparisons of amplitude and phase between adjacent beams. In this radar, the transmit signal is transmitted through each of 4 antennas simultaneously.

Figure 11 shows the normalized antenna diagram implemented by the LRR system with four antennas with superimposed beams. It can be observed that each lobe has about 4 degrees of -3 dB bandwidth and it has an angular coverage of about 16 degrees. The specifications of this radar show 28 dBi of average gain.

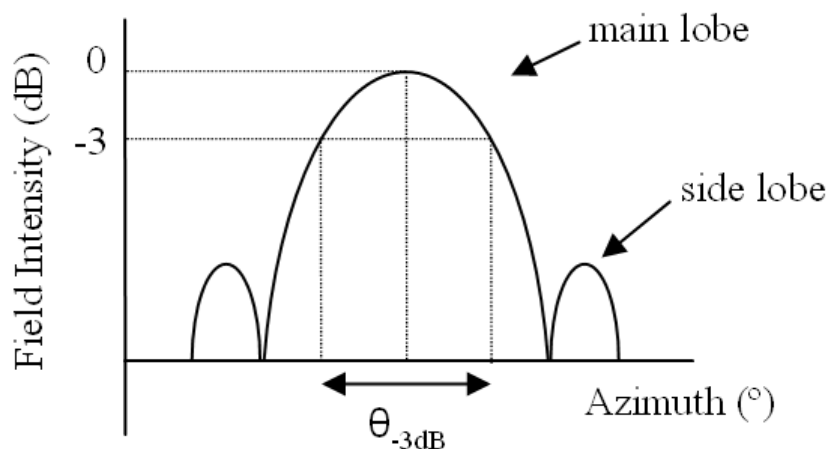


Figure 10. Example of antenna diagram.

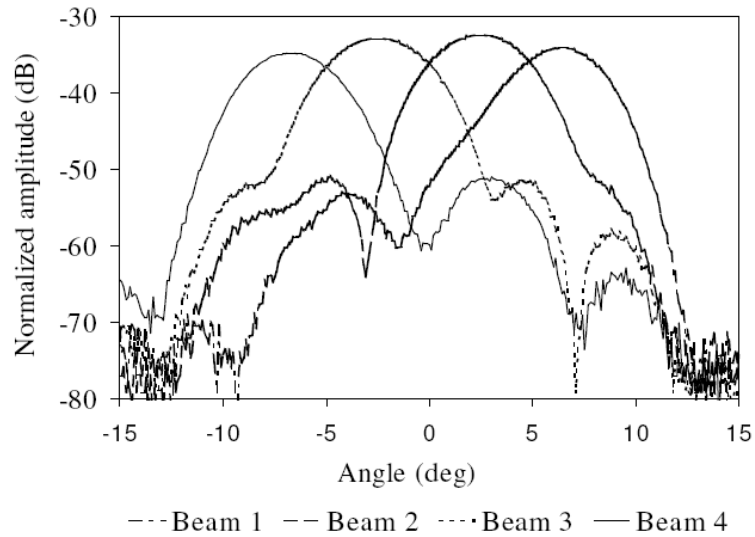


Figure 11. Antenna diagram of LRR2 [36].

4.3 FMCW Signal

As this radar is produced by an automotive application, ACC, the parameters of the FMCW signal are optimized to detect cars. For this reason, in order to understand the results in the measurements, the signal emitted is analyzed.

FMCW radar transmits a continuous wave signal which frequency is modulated as a function of time with a periodic wave form presented in order to generate three linear frequency ramps with different ramp times and bandwidth as show the *Figure 12*. The ramps 1 and 2 each have 180 MHz of bandwidth and 1.4 ms of duration, while ramp 3 has 200 MHz of bandwidth and 6.6 ms of duration.

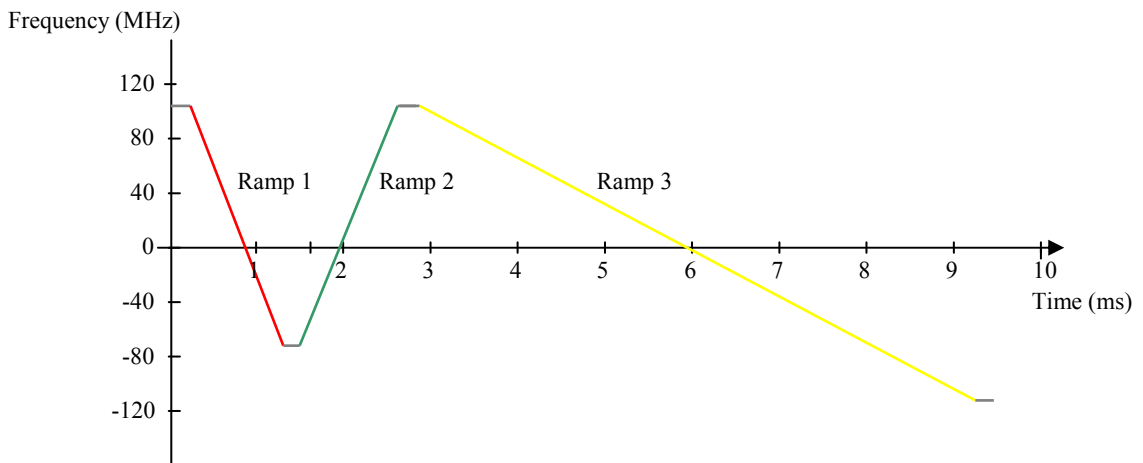


Figure 12. FMCW signal transmitted by LRR2[36].

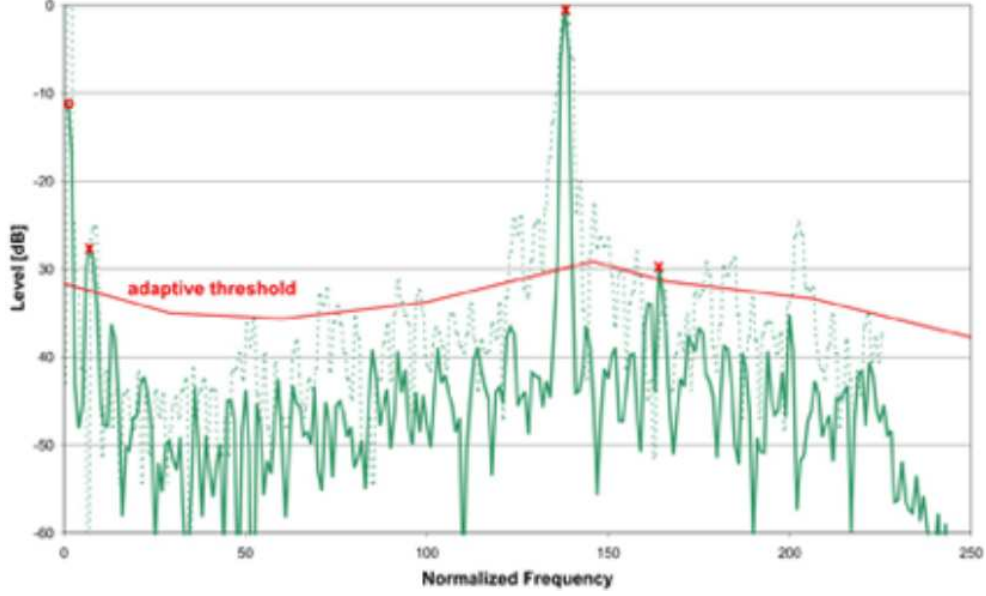


Figure 13. Spectrum of an intermediate frequency[36].

As stated previously, the signal is transmitted through each of the four antennas. The received signal is also acquired by each antenna. Each signal is then mixed with a current signal to form an intermediate frequency. This represents twelve intermediate frequencies: one for each ramp in each antenna.

Each intermediate frequency is sampled with a sampler frequency f_s in the ADC and then is processed through a DSP using FFT algorithms with a window of 256 samples. *Figure 13* shows an example of an intermediate frequency, presenting and adaptive threshold that is used to exclude potential objects. The peaks marked with a red x are considered objects and are processed to determine their position.

4.4 Detection Characteristics

Once the beat frequencies are obtained, each of these frequencies has to be related with an object at a certain distance with certain velocity. As stated in *Section 2.4*, the beat frequency can be expressed in function of radial distance and radial speed. For this, radar resolves mathematically the following equations in order to obtain the distance and speed of the object detected:

$$f_{b-}^1 = f_r + f_d = \frac{2\Delta f_1}{c\Delta t_1} r + \frac{2f_0}{c} v \quad (4.1)$$

$$f^2_{b+} = f_r - f_d = \frac{2\Delta f_2}{c\Delta t_2} r - \frac{2f_0}{c} v \quad (4.2)$$

$$f^3_{b-} = f_r + f_d = \frac{2\Delta f_3}{c\Delta t_3} r + \frac{2f_0}{c} v \quad (4.3)$$

where Δf_i indicates the sweep frequency and Δt_i the sweep time in the ramp i during the positive slope in the *Equation 4.2* and during the first and third negative slope in the *Equation 4.1* and *Equation 4.3* respectively, accordingly with *Figure 12*.

In order to understand the advantages of using a transmitted signal composed of three ramps, the measurement protocol of a radar that sends a signal is composed of one, two and three ramps is explained next. Considering first a FMCW radar which uses only one ramp in the transmitted signal, the radar has to resolve one of the three previously mentioned equations. Representing this equation in a distance/speed diagram in *Figure 14* for an object at 40 m and 25 m/s it can be observed that the solution is a line with multiple pairs of distance/velocity results instead a point.

The reason for this is that the radar has only one equation and two unknowns. For this, the acquisition of speed and distance information is non possible. This solution is only useful to detect distance information in non-moving targets.

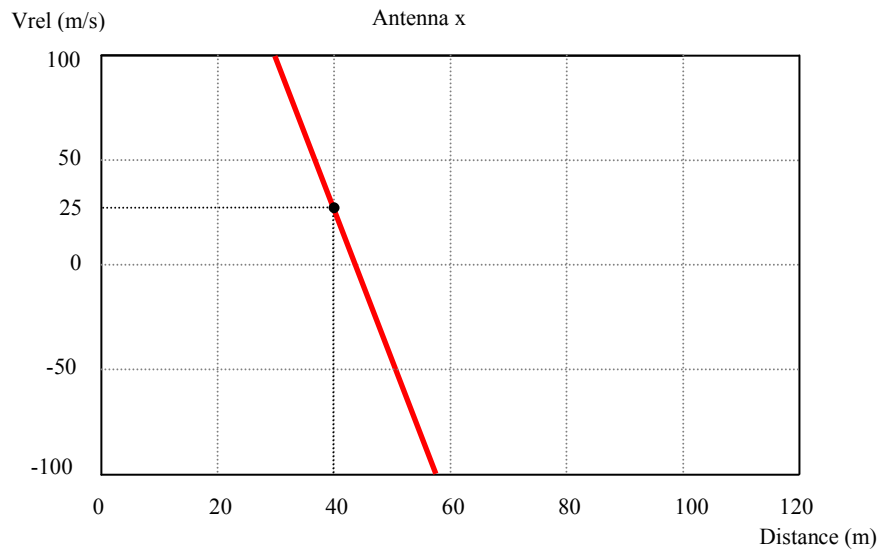


Figure 14. One moving target at a distance of 40 meters with 25 m/s of velocity represented solving Equation 4.1 (redrawn from [36]).

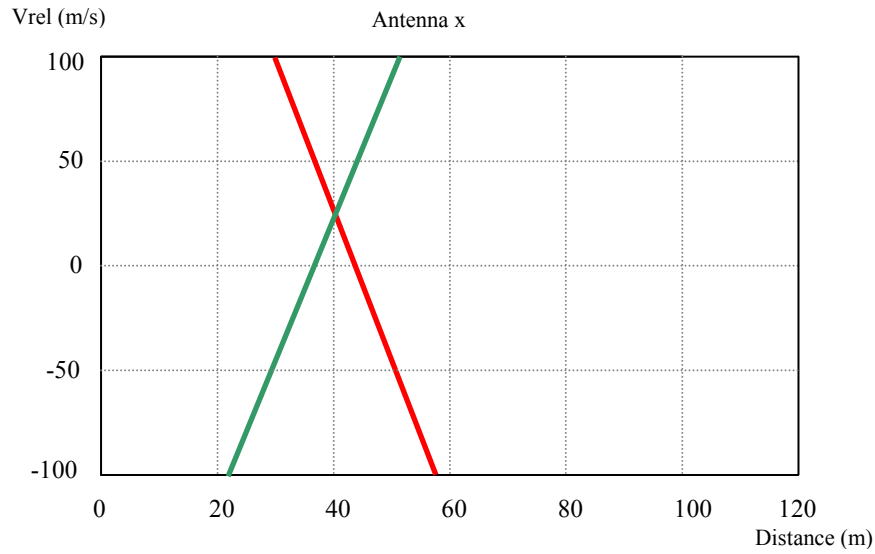


Figure 15. One moving target at a distance of 40 meters with 25 m/s of velocity represented solving Equations 4.1 and 4.2 (redrawn from [36]).

Considering now a FMCW radar which transmits a signal formed by two ramps with negative and positive slopes, the radar has two equations to resolve two unknowns. Representing the same object in a distance/speed diagram using both equations in Figure 15 it can be seen as the solution of these equations are two lines with multiple pairs of distance/velocity results, but only the point where there is the intersection of the two lines is the correct result. Considering now that more than one moving target is present in the range of coverage, the distance/velocity diagram produced by three moving targets at different distances and speeds would therefore be:

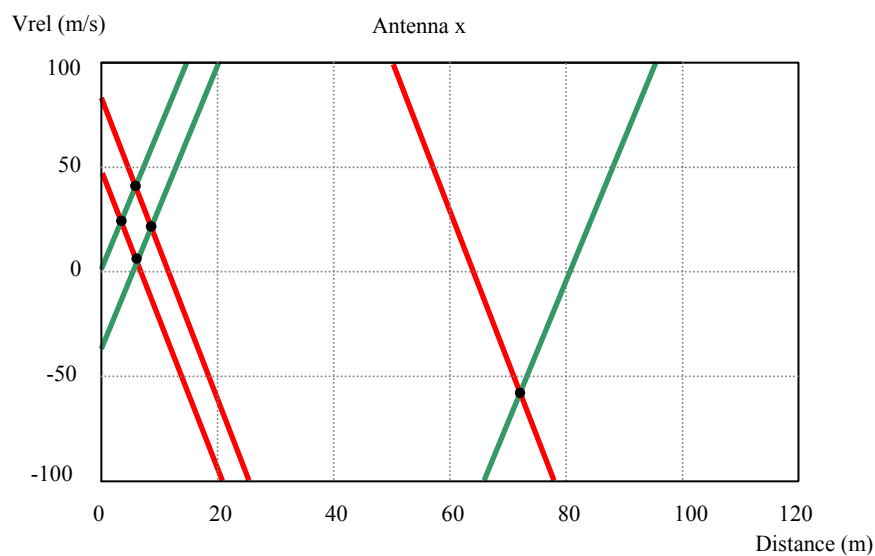


Figure 16. Three moving targets at different distances and different velocities solving Equations 4.1, 4.2 and 4.3 (redrawn from [36]).

As can be seen in *Figure 16*, there are five points where the lines intersect. However, there are only three moving objects. With this diagram, the radar will deem that there are five objects.

In order to avoid the detection of virtual objects (also known as ghosts), the modulation scheme has to contain an additional ramp with a different slope to that of the first two ramps. However, this additional ramp increases the complexity of the signal processing. *Figure 17* shows the same objects that were presented in the previous figure but using an additional ramp.

Using the third ramp, an object is deemed detected if lines of all three ramps intersect at a point on the distance/velocity diagram. As shown the *Figure 17*, there are only three points where the lines intersect corresponding to the three real objects. For this, in a multiple target environment, there is the need to use three ramps in the FMCW signal.

Using a three ramp signal, however, due to reflections in the same object or due to closer objects, virtual objects may also appear. For this reason, the probable sequences of locations are predicted on the basis of the continuity of the movement using the knowledge acquired in the previous calculations of the detected objects. The superposition of this information obtained for each of four antennas makes it possible to obtain, moreover distance and velocity information, as well as angular position.

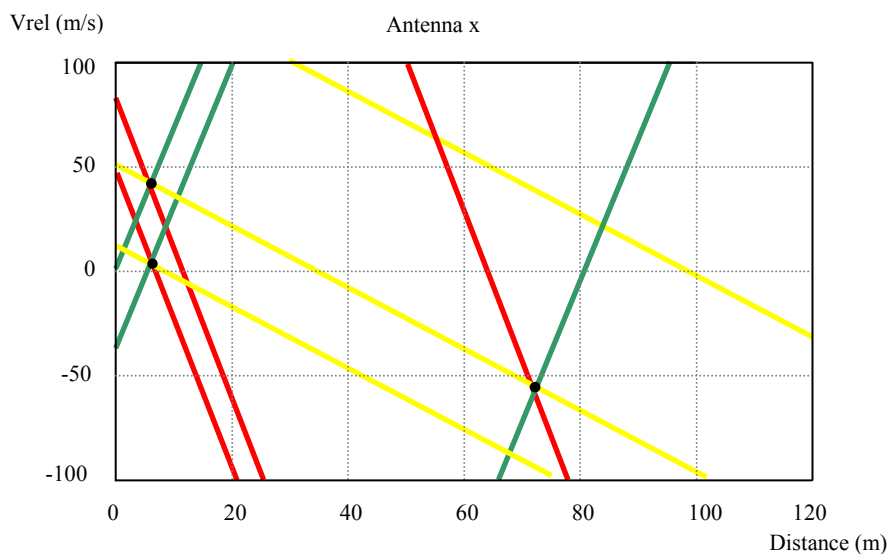


Figure 17. Three moving targets at different distances and different velocities using an additional ramp (redrawn from [36]).

4.5 Range Resolution Degradation in the Receiver

In FMCW radar systems, range resolution depends on the transmitted bandwidth, the processed overlap between the transmitted and received frequency sweeps, the receiver frequency resolution and the frequency sweep linearity. As the manufacturer does not provide information about the frequency sweep linearity, this section only take the receiver range resolution into account [28].

The ideal range resolution ΔR_0 is linearity proportional to time resolution ΔT and inversely proportional to the transmit time waveform bandwidth ΔF for any radar waveform, as given below:

$$\Delta R_0 = \frac{c\Delta T}{2} = \frac{c}{2\Delta F} \quad (4.4)$$

For example, a FMCW radar waveform with 180 MHz total frequency deviation has the potential for range resolution no less than 0.83 m.

Considering from now the ramp 1 in the FMCW waveform with the characteristics described in Section 4.3, the maximum beat frequency will be when both range and velocity will be maxim, then:

$$f_b = f_r + f_v = \frac{\Delta f_1}{t_1} \frac{2}{c} R_{\max} + \frac{2}{\lambda} v_{\max} \quad (4.5)$$

According to the specifications of the radar shown in Appendix, for a maximum range of 200 m with a velocity of 60 m/s, the maximum beat frequency is:

$$f_b = \frac{180 \cdot 10^6}{1.4 \cdot 10^{-3}} \frac{2}{3 \cdot 10^8} 200 + \frac{2}{3.92 \cdot 10^{-3}} 60 = 202 \text{ KHz} \quad (4.6)$$

In order to satisfy the Nyquist criterion, the ADC sampling rate must be at least two times the maximum beat frequency:

$$f_s \geq 2f_{b_{\max}} \quad (4.7)$$

The portion of the modulation period during which the beat frequency is within the receiver bandwidth is less than 1.4 ms. Considering the sampling frequency as $f_s = 2f_{b_{\max}} = 404 \text{ kHz}$, the time that the ADC need to sample 256 samples as the FFT need take:

$$t = \frac{256}{f_s} = 0.63 \text{ ms} \quad (4.8)$$

and as can be seen in this time is shorter than the duration of the ramp 1.

Performing a 256 point FFT on those samples yields a bank of filters from 0 to 404 kHz with each 1.58 kHz frequency bin corresponding to a 1.84 m range bin. Using the Hamming window to reduce the frequency and range side lobes results in 6 dB resolution of 1.81 bins [29], corresponding to 2.86 kHz receiving frequency resolution. Finally the range resolution becomes 3.33 m.

Chapter 5

Measurements

The manufacturer provides the specifications and limitations of the radar for targets that are vehicles. Thus, the characteristics and limitations with human targets have to be determined. In order to define these characteristics, first of all, the measurements of detection range, *Field Of View* (FOV) and range resolution are performed in a flat open area (a football field). The FOV is the area in which the radar is able to detect targets. The FOV is usually expressed in degrees (both elevation and azimuth). Afterwards, different measurements in a real environment are realized. Finally, a comparison between automotive radar specifications and the measurements with humans is made.

5.1 Introduction

The sensing system consists of a long range radar placed in the front of the car, with embedded ACC algorithms. As the radar detects and tracks objects with its field of view, real time target data are transmitted over the Controller Area Network (CAN) bus to the laptop for data collection and display purposes. The CAN bus is a vehicle bus standard designed to allow microcontrollers and devices to communicate with each other within a vehicle without a host computer. *Figure 18* shows the car used in the measurements which recorded data from the radar placed behind the car insignia.

Using an application developed in Matlab, the data are presented as shown in *Figure 19*. On the upper left hand corner, each detected target is displayed as a red point on the map. On the upper right hand of the display, each target is represented with a target identifier, x position, y position and radial velocity. These data are saved in a text file for posterior analysis as well.



Figure 18. Test vehicle with 77 GHz LRR inserted in the car insignia.

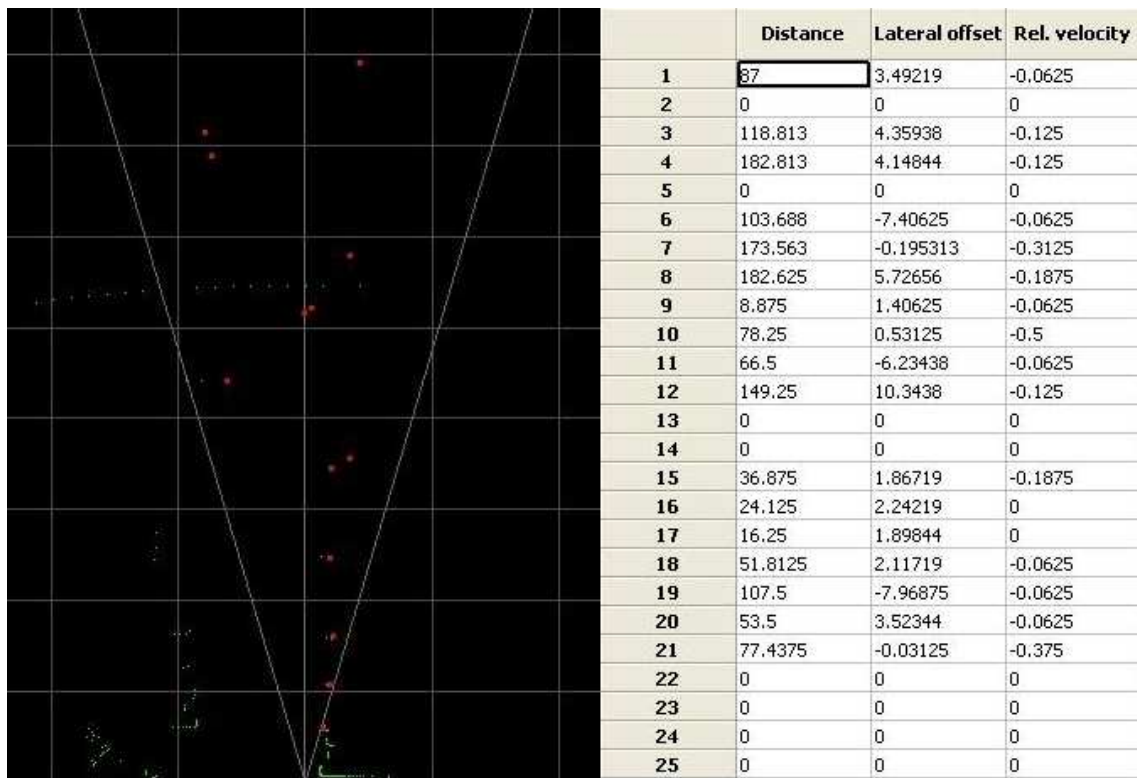


Figure 19. Matlab application to present the target information on the laptop.

The measurements were divided into two parts. The first measurements were aimed at determining the limitations of this radar when the target is a human. In order to estimate these limitations the signal received by the radar had to be due only to a human target. For this reason the chosen area had been a football field where there was a sufficiently large and flat open area with no interferences due to another types of targets.

Once the basic characteristics are defined it is important to move the measurement field to a real environment, where different types of targets are present. For this reason, the goal of the second part of the measurements was to check the ability of the radar to detect humans when they are walking around cars, trees, buildings, traffic signs and other obstacles.

Both measurements are realized during daytime on a sunny day with an ambient temperature around 10 degrees. The presence of bad weather conditions such as rain, snow or fog, however, should not affect the measurements as is demonstrated theoretically in Section 2.7.

5.2 Maximum Range and Range Accuracy

According to the specifications (see Appendix) the maximum range of the LRR2 is 200 meters and the range accuracy is 0.5 meters, when the target is a vehicle. In this section, both parameters are determined for human targets. *Figure 20* shows the football field where these measurements are realized. Also visible is the measuring tape on the ground to check the range accuracy of the radar.



Figure 20. Football field where radar measurements is made.

The first step was to perform a rough estimate of the detection range with human targets. For this, one human started to walk away from the radar. The location became uncertain and approximately the 50% of the time the target disappeared at about 80-90m. Thus, it was decided to make the measurement area 100 m long.

In order to calibrate the range of the radar, the range of a human standing at specific range points are measured by the radar and is compared with the same distance measured with a measuring tape, as shown the *Figure 21*.

Table 3 shows the results of the range calibration. It is interesting to note that in all twelve measurements the radar range accuracy is better than the 0.5 meters mentioned in specifications of the radar. Another important finding is that there is no increase in the radar range error proportional to the range. The average of errors at different distances is 14 cm.

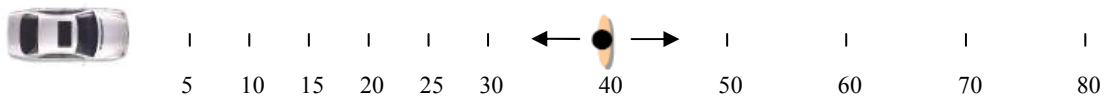


Figure 21. Measuring method illustration for range accuracy.

Table 3. True range versus radar range at different distances. True range is the range measured with a measuring tape, Radar range is the range measured by the radar, Error is the difference between True range and Radar range expressed in % (in respect to True range) and in meters.

True range (m)	Radar range (m)	Error (%)	Error (m)
5.00	5.00	0.00%	0.00
10.00	9.87	1.32%	0.13
15.00	14.94	0.40%	0.06
20.00	19.81	0.96%	0.19
25.00	24.94	0.24%	0.06
30.00	30.00	0.00%	0.00
40.00	39.87	0.33%	0.13
50.00	49.75	0.50%	0.25
60.00	59.87	0.22%	0.13
70.00	69.69	0.44%	0.31
80.00	79.81	0.24%	0.19
90.00	89.81	0.21%	0.19

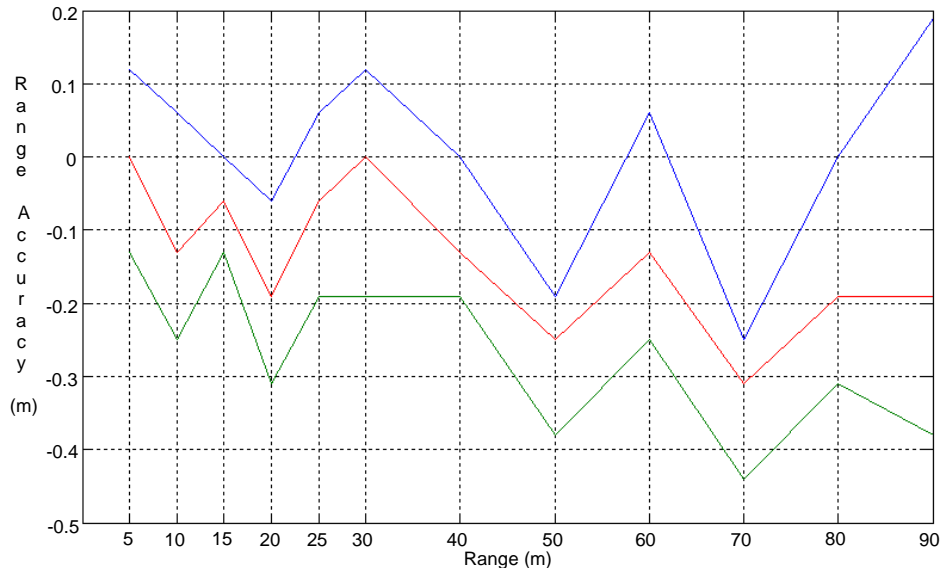


Figure 22. Behaviour of the measurement error with distance. The blue line represents the maximum error, the red line the average error and the green line the minimum error.

The observed range accuracy was very satisfactory compared with the specifications, however, another important result is that the measurements provide information about the noise of the measurement. Figure 22 shows the maximum and minimum accuracy values and the average accuracy as well. As can be seen, except the measurement at 90 meters, the maximum and minimum error value is less than 0.5 m.

In order to determine the maximum range where a human can be detected, a human target walks away from the radar along the centre of the FOV until the target disappears from the radar screen. Next, the human target goes to a distance where the radar is not able to detect them and then starts walking towards the radar. The same measurement is performed also for both sides of the FOV. Table 4 shows the maximum distance where the radar is able to detect the presence of a human.

As can be seen these values are different when a human target is walking away and towards to the radar. Whereas the maximum range is higher when a human is walking away to the radar at the center of the FOV, this value is higher when a human is walking towards the radar at the both sides of the FOV.

Table 4. Distance where the human target is walking towards and away from the FOV can be detected.

	Left side (m)	Center (m)	Right side (m)
Walking away	90.20	93.40	91.00
Walking towards	94.60	87.60	93.60

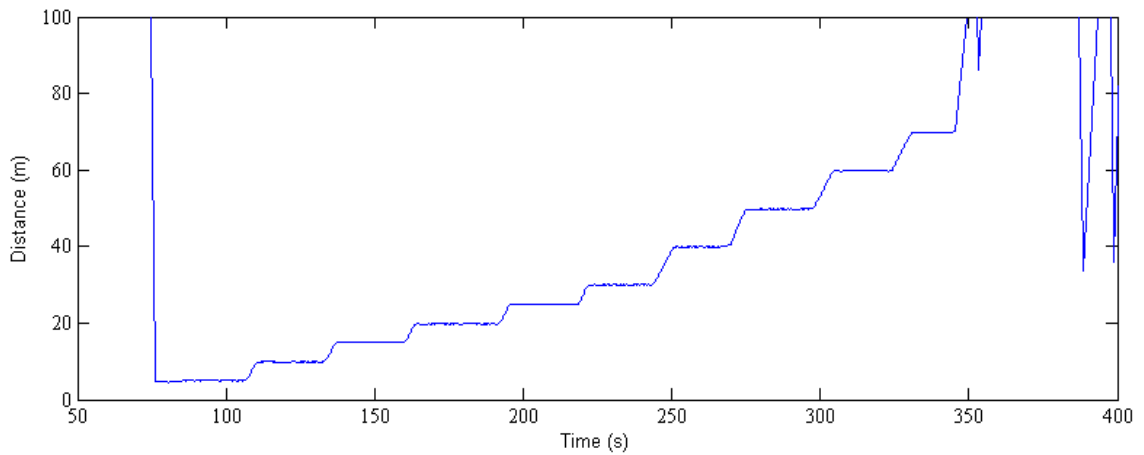


Figure 23. Distance (Range) to a human target walking on the football field during the measurements. When the distance is above 70 m he radar loses the lock on the target.

The radar range accuracy is very satisfactory compared with specifications up to distances of 90 meters and the radar is able to detect the human's presence when a person is walking away and towards to the radar up to 90 meters approximately, however, the radar is not able to follow a human at this distance. As can be seen in *Figure 23*, which shows the human behaviour tracked by the radar during the accuracy in range measurements, the radar can follow a target up to about 70 meters without loosing the lock on the target.

5.3 Maximum Field of View

The second step after measuring the maximum range and range accuracy is the FOV measurement. This measurement will allow the determination of the effective area where the radar is able to detect humans. In order to estimate the true shape of the FOV, a radar reflector shown in *Figure 24* is used.

This trihedral reflector is made of 3 flat surfaces arranged to form a corner with the sides intersecting at 90°. When radar energy strikes one of these surfaces it is usually reflected back along the same direction (to the antenna) via the other two surfaces. Reflectors are usually used to fix the limitations of a radar as they has a high RCS. The procedure to determine the FOV is to measure the maximum distance on both sides of the center line where the radar is able to detect a target at a given range, as shown *Figure 25*.

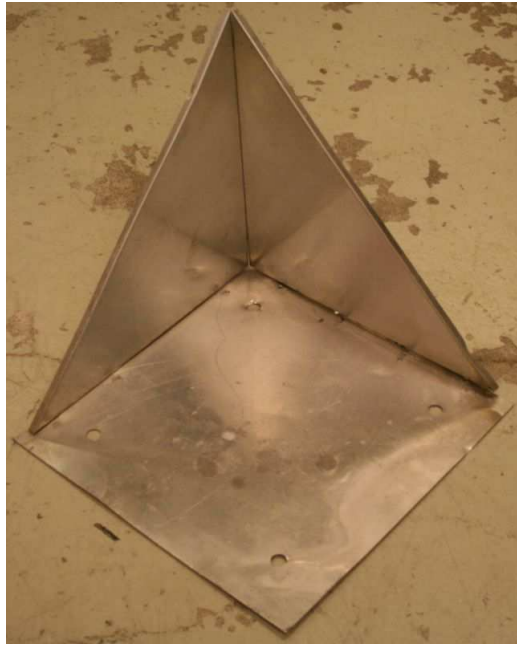


Figure 24. Trihedral Reflector used to estimate the FOV.

The reflectors are moved from the centre line to the sides at specific range points, until they disappear from the radar screen. Then, they are brought back until they reappeared. This procedure is also used with a human target to estimate the real FOV in human detection. The results using radar reflectors and humans are shown in *Table 5*. The FOV can then be easily calculated by using the distance of the target from the center line, the distance of the center point from the radar and a simple trigonometric equation.

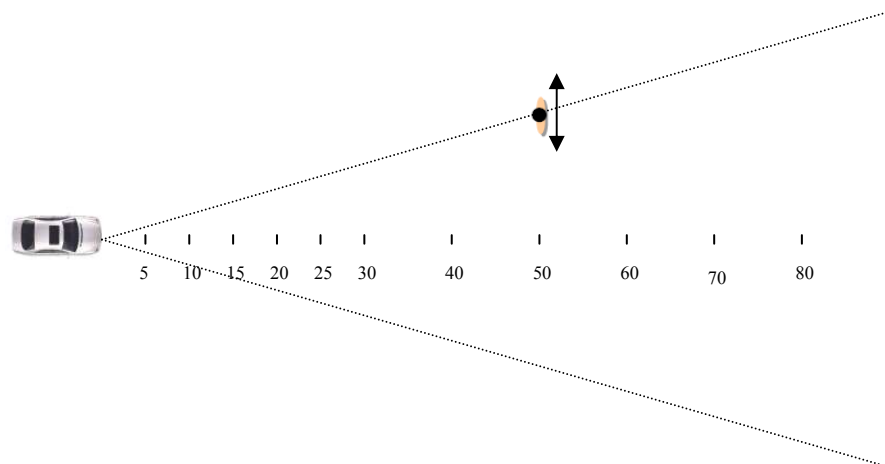


Figure 25. Measuring method illustration for FOV.

Table 5. Distance measurements to determine the FOV using a radar reflector and a human.

Radar Reflector					
True range (m)	Distance left (m)	Distance right (°)	FOV left (°)	FOV right (°)	FOV (°)
30	5.5	4.9	10.4	9.2	19.6
50	7.9	8.5	9.0	9.7	18.7
80	12.5	12.5	8.9	8.9	17.8

Human					
True range (m)	Distance left (m)	Distance right (°)	FOV left (°)	FOV right (°)	FOV (°)
15	1.5	2.0	5.7	7.6	13.3
30	3.5	4.0	6.7	7.6	14.3
50	5.0	5.0	5.7	5.7	11.4

As was expected, the FOV using a radar reflector is larger than when a human is the target, since the RCS of the radar reflector is larger. With radar reflectors, the FOV is approximately 18°, which is larger than the value in the specifications of the radar. However, with a human target this value will decrease to approximately 13°.

5.4 Angular resolution and Angular Accuracy

The third step is to fix the angular resolution in human targets and its accuracy. Angular resolution is the ability of the radar to separate two human targets when they are at the same radial distance but in different position. Angular accuracy is specified as the error that the radar makes in the measurement of the angular position. For this reason, the humans are at the specified points and start moving away from each other, as shown *Figure 26*. The minimum separation when both targets are detected as separate targets is measured with measuring tape and radar.

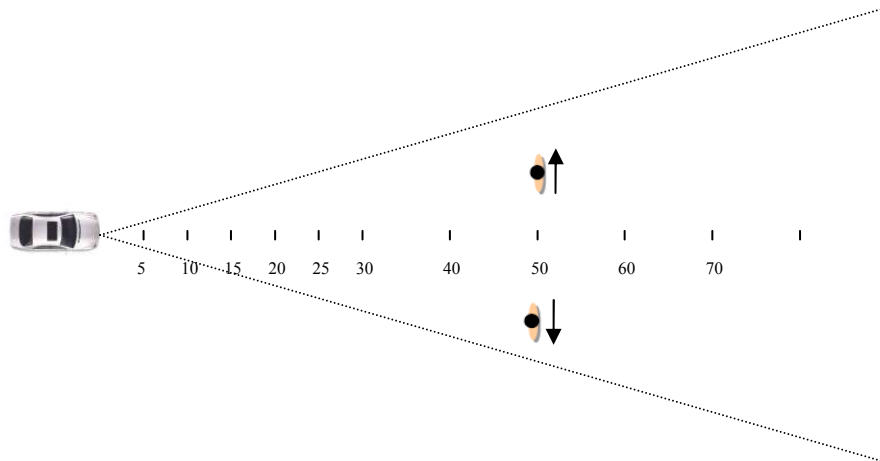


Figure 26. Measuring method illustration for angular resolution and accuracy.

Table 6. Minimum distance between human targets when they are detected as separate targets as a function of range. Radar separation is the distance between the targets measured by the radar. True separation is the distance between the targets measured with the measuring tape. Angular resolution is calculated using the radar separation. Angular error is the difference between angular resolution and the angular resolution calculated through the true separation.

True range (m)	Radar separation (m)	True separation (m)	Angular resolution (°)	Angular error (°)
15	Targets are not separated			
20	4.4	4.5	12.84	0.29
25	4.5	4.8	10.97	0.68
30	6.5	6.3	11.99	0.38
40	7.5	7.6	10.71	0.14
50	10.0	10.1	11.53	0.11

The results are shown in Table 6 and it can be seen that two human targets cannot be separated when the range is less than 20 meters. The value of the angular resolution is close to the maximum FOV, so the radar is only able to separate two humans at the same radial distance when they are at the edge of the FOV.

5.5 Range Resolution

Finally, in order to finalize the measurements, the range resolution of the LRR is checked in different scenarios. The range resolution is the ability of the radar to detect two close targets at different radial range. The range resolution between two humans is determined first, and then, the range resolution between humans and different targets as well. These targets are chosen taking the size and material into account. The method used to fix the range resolution between two humans is shown in Figure 27. Two humans at different range in the center of the FOV start to move from each other, and the minimum distance which they are detected as two targets corresponds to a range resolution.

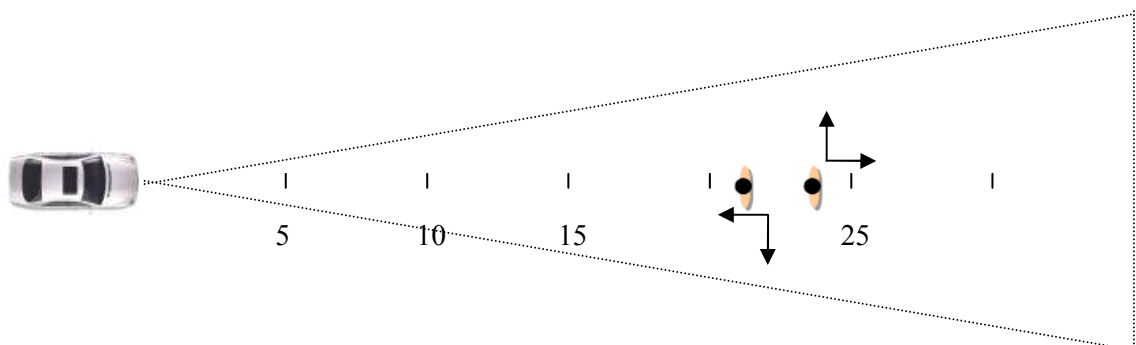


Figure 27. Measuring method illustration for range resolution between humans.

Table 7. Range resolution between two humans, where human 1 and 2 are the radial distances measured by the radar, radar separation is the difference in distance between both humans measured by the radar and error is the difference between the Radar separation and the separation measured with a measuring tape.

Human 1 (m)	Human 2 (m)	Radar Separation (m)	Error (m)
15.0	14.0	1.7	0.3
23.0	21.0	2.0	0
25.0	22.0	2.8	0.2

Table 7 shows the range resolution between two humans at different ranges. As can be seen, the range resolution increases (becomes poorer) with the distance from the radar. These distances are clearly smaller than those shown in Table 6 due to the difference between the range resolution and angular resolution.

Unlike in the previous measurements which have been realized in a flat open area with only human targets, the next measurements have been realized with different types of objects in the FOV.

In order to evaluate the behaviour of the radar when a big metal target with a larger RCS is close to the human, the measurement shown in Figure 28 is realized. The distance between the car and the radar is 30 m. When a human target starts to walk away from the car towards the radar, it is detected as a separate target at a distance of 3.7 m from the car. However, when the human walks sideways away from the car he is not detected at all. Thus, the radar system can more easily detect targets that have different ranges than those that are in the same range as a consequence of the smaller angular resolution measured in Section 5.4.

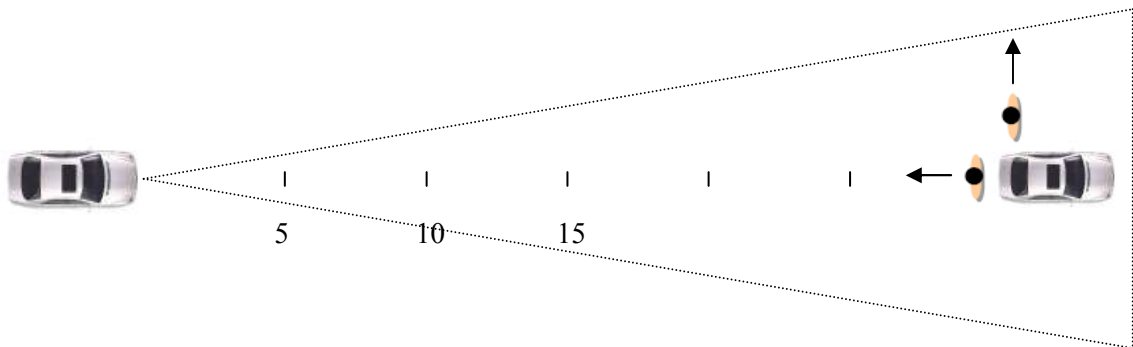


Figure 28. Measuring method illustration for range resolution between human and car.

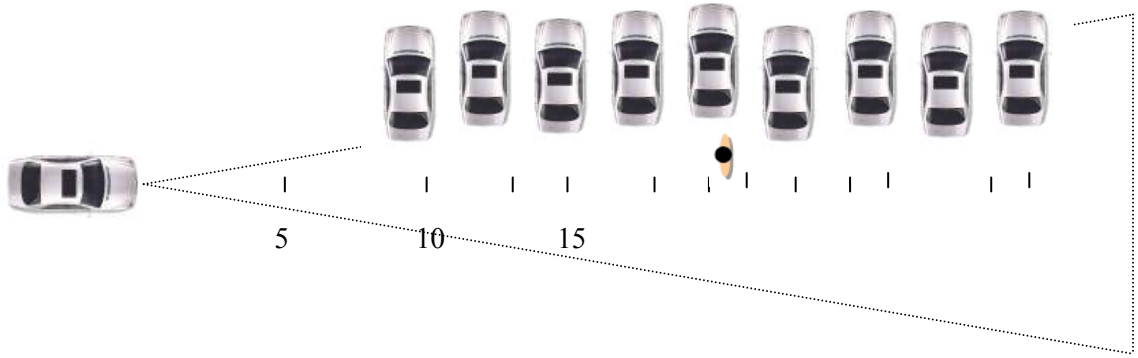


Figure 29. Measuring method illustration for range resolution between a row of cars and human.

In the next measurement the radar was placed so that the FOV was parallel to a row of cars in the parking lot as shown *Figure 29*. The human walking from between the cars to the FOV was quickly detected. Only those cars that were more visible were detected as targets by the radar. The parallel cars have a smooth surface which involves a smaller RCS that does not affect the detection significantly.

The next objective was to check the range resolution when a wall made from bricks and concrete is behind or next to the human target. The first measurement setup is shown in *Figure 30a*. The radar is positioned so that the wall is in the FOV of the radar. A human walking along the wall was detected by the radar regardless of the distance between the human and the wall. Also, when a human appeared behind the corner into the FOV he was quickly detected. The ranges tested were up to about 20 meters. The parallel wall has a smooth surface which does not affect the detection significantly.

Next a measurement setup with the wall behind the human was tested as shown in *Figure 30b*. With this configuration the wall affected the detection. The human was detected as a separate target only when there was some distance between him and the wall as shown by *Table 8*. The distance needed between the wall and the human increased with range.

Table 8. Distances when a human was detected as a separate target from the wall behind him for three ranges (from the radar to the wall).

Range (m)	Distance between human and wall (m)
10	2.6
20	3
46	4.2

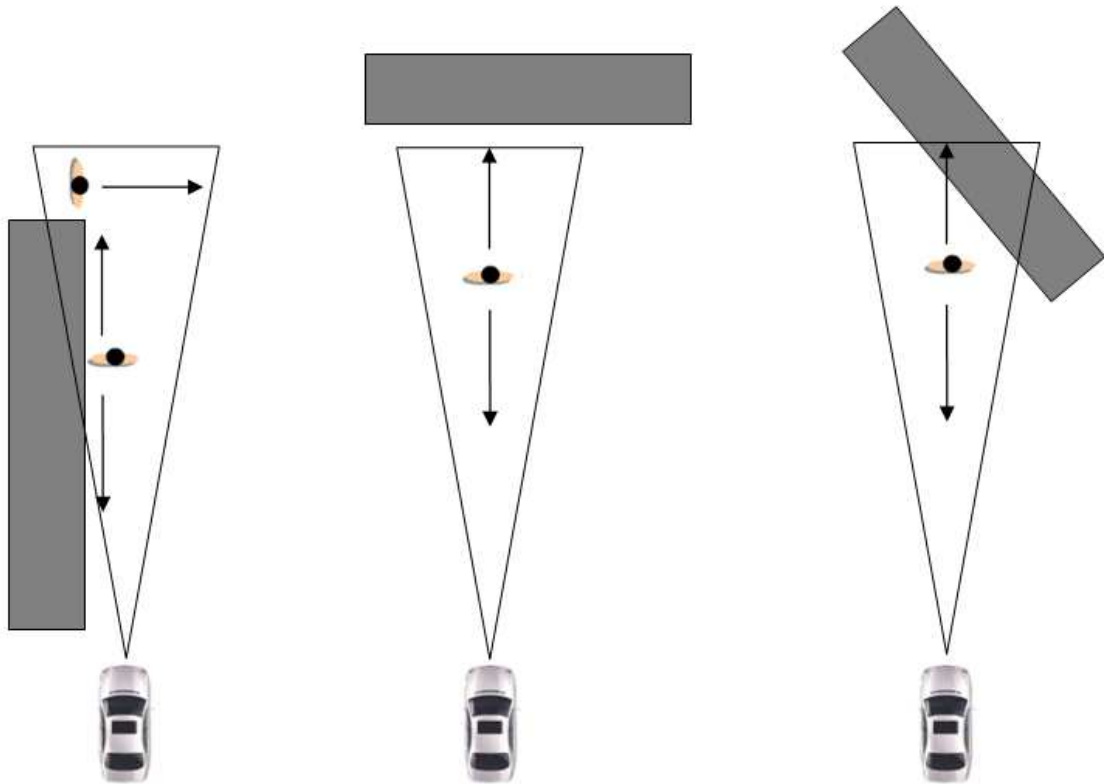


Figure 30. From left to right: a) Measurement method illustration with a wall parallel to the FOV of the radar. b) Measurement method illustration with a wall behind the human. c) Measurement method illustration with a wall at 45 degree angle.

The third measurement setup was with a wall at approximately angle of 45 degrees angle shown in *Figure 30c*. At a range of 9.25 meters from the wall, the human was detected as a separate target when there was a distance of 3 m between the wall and the human.

In the last measurements a tree and a traffic sign was in the FOV of the radar and its effect on the detection of a human was measured. For this, in *Figure 31a* a human was placed close to a traffic sign and in *Figure 31b* a human walks around trees.

Trees were detected by the radar. However, their radar cross-section seemed to be smaller than that of a human. When a human walked towards a tree the radar was “locked” on the human and the location marker of the tree was merged to the human when the human was close enough, opposite to what happened with the wall, cars and other large targets. When the human walked sideways away from the tree the signal was slightly ambiguous. Usually the radar tracked the human but sometimes it tracked the tree.



Figure 31. a) Measurement place to observe the behaviour of the radar with traffic signs. b) Measurement place to observe the behaviour of the radar with trees.

When the tree was at the edge of the radar screen, however, it was easier to track the human. The hypothesis is that objects at the center of FOV are the preferred targets to the radar (or perhaps the signal is stronger there). The radar cross-section of a traffic sign seemed stronger than that of a human. At a range of 18 meters a human was detected as a separate target when the separation distance along range direction was 3 m whereas at a range of 10 m the needed separation was 2 m. When a human moved sideways away from the radar he was not detected at all (same as with the car measurement above).

5.6 Conclusions

The measurements realized in this chapter provide the real limitations of the LRR2 in human detection. As was expected, the differences between the specifications with the measurements obtained during testing are considerable. For example, the maximum detection range has decreased from 200 meters to only 90 meters and the radar is only able to track (have the same target ID number) a human to 70 meters. The accuracy in range, however, is better than the specifications. However, all the measurements were performed with stationary targets. The range error may increase when the radar and/or

the target is moving. In addition, one of the most important characteristics of the radar, the FOV has been also reduced to 13° (from 16°). These limitations have reduced the zone of coverage from 2800 m^2 to approximately 280 m^2 (considering a maximum range of 70 meters). The main reason for this is that the human has a RCS smaller than a car.

One of the problems observed in the measurements is the difficulty of the radar to separate two humans at the same longitudinal distance but with different transversal distances. However, when they are at different longitudinal distance, the radar has not these limitations. The poor angular resolution could be the problem in this case.

When a human is close to an object with a larger RCS, the radar has severe problems to detect the human. In the measurements this behaviour was observed when a human is close to a car, wall, trees or traffic signs. The results shown that the range resolution between humans and other objects with larger RCS increase with the range. At a distance of 30 m, a human can be detected as a separate target from a car with a range resolution of 3.7 m.

Chapter 6

Improved Radar Techniques for Human Detection and Identification

The radar used in the measurements was not optimized for detecting humans. While humans are detected as targets, the output data of the radar does not indicate whether they are humans or other obstacles. In this chapter various more advanced radar technologies are described and their potential for human identification is discussed.

6.1 Synthetic Aperture Radar System

Synthetic Aperture Radar (SAR) is a type of radar or method that improves natural radar resolution by analyzing the signal received through a process known as synthetic aperture processing. Whereas the traditional radars transmit directional pulses of electromagnetic energy and detect the presence, position and movement of a target by analyzing the portion of energy reflected from the target, SAR attempts to form an image of the target area as well.

The most important characteristic of SAR is that it uses the movement of the platform where the radar is fixed to take many samples of the same target from different points. As a result the antenna works as a virtual antenna with a greater aperture size. The amount of measurements acquired for each target is dependent on the size of the synthetic aperture, and as a consequence, the resolution acquired is similar to a real aperture antenna of the same size.

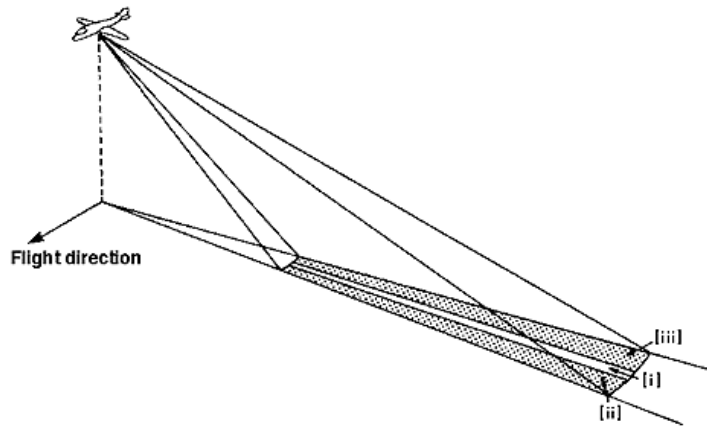


Figure 32. SAR measurement technique [37].

In the field of human detection, SAR possesses the advantage of the radar technology and not only detects targets but also can make a picture of the whole field of view. However, it requires complex computing processing to be done in real time. The main problem with SAR, however, is the basic principle of SAR. As can be seen in *Figure 32*, SAR can only measure a surface that is parallel to the movement direction of the radar (i.e. on the side of the radar), and in human detection there is the need to also measure the area in front of the radar.

6.2 Polarimetric Radar

The different types of radars described until now transmit and receive electromagnetic waves with horizontal or vertical orientation, in other words, the electric field wave crest is oriented in the horizontal or vertical direction. The main characteristic of polarimetric radars, also called dual-polarization radars, is that they transmit electromagnetic waves with both horizontal and vertical orientation. As a result, polarimetric radars are able to obtain information of the horizontal and vertical dimension of the target. This additional information can be decisive in some applications to improve the accuracy.

Figure 33 shows the human reflectivity between 0.9-20 GHz in horizontal and vertical polarizations [30]. These measurements have been made with an *Ultra WideBand* (UWB) radar at a distance of about 2.6 m from a human and the main goal of the measurements was to develop a sensor that can detect the motion due to breathing.

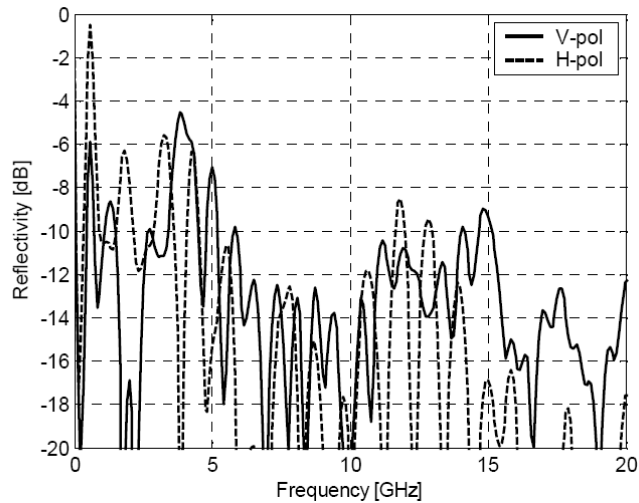


Figure 33. Reflectivity of a human body with vertical and horizontal polarization in a range of 0.9-20 GHz [30].

Some important differences between both polarizations along the frequency range can be observed. For example, there are frequencies where there is a maximum reflectivity in one polarization and a minimum in the other. However, the polarization signal is very sensitive to the shape and position of the target and also the clothing and any metal object (e.g. tools) carried by the human will affect the signal. Thus, more measurements are needed in order to test if the polarization signal is usable as method for identification purposes in more complex situation.

6.3 Dual Band Radar

The backscattering characteristics of a target are included in its RCS. The RCS of the target often depends on the frequency that is used. Thus, the basic idea of a dual band radar is to use the difference in the power of the signal reflected from an object at different frequencies to recognize which type of object it is. Figure 34 shows the receiving rates of iron and the human hand within a range from 10 to 60 GHz. The solid line represents the receiving rate which is equivalent to the division of receiving energy and transmitting energy whereas the dashed line represents the ratio of receiving rate which is equivalent to the division of receiving rate at 10 GHz and the receiving rate of each frequency [32].

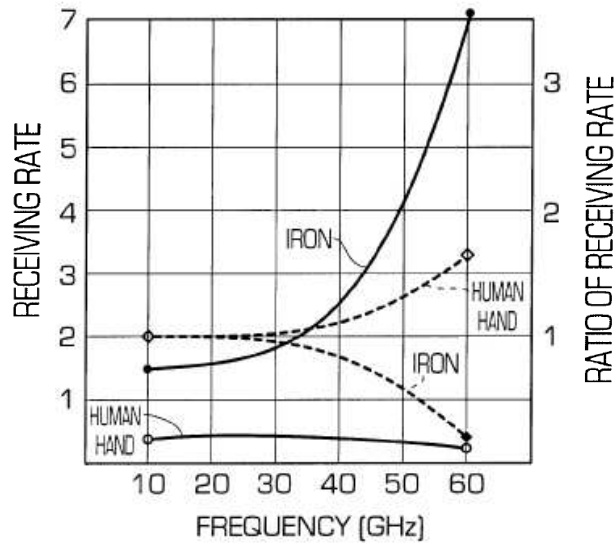


Figure 34. Receiving rates of iron and hand within a range from 10 to 60 GHz [32].

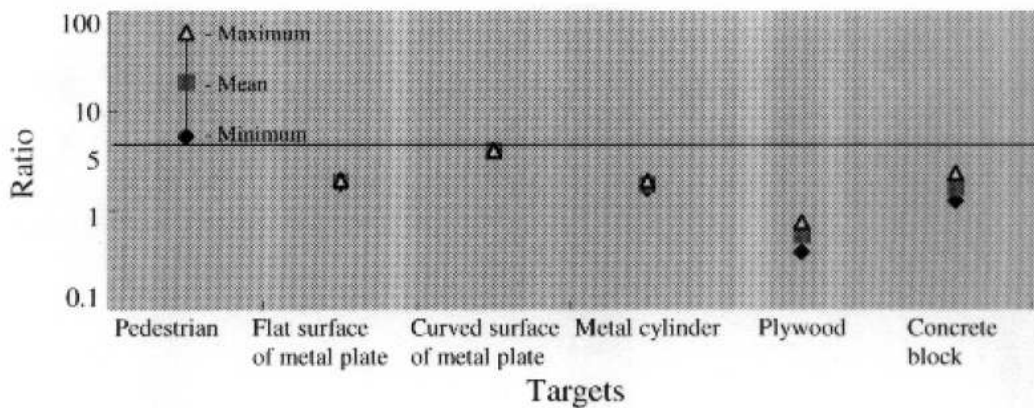


Figure 35. Maximum, minimum, and average values of ratio for different targets [33].

As can be observed in *Figure 34*, the receiving rate of iron increases exponential with the frequency whereas the human hand decreases slowly. However, considering the ratio of receiving intensity between two frequencies away from each other, the information content is higher. This way, we have more accurate information about the object, and by comparing the rate the target identification can be made.

A radar system using two FMCW radars at 10 GHz and 60 GHz to distinguish pedestrians from other objects using the dependence of the characteristics of the backscattered energy from a human in both frequencies is presented in [33]. As can be seen in *Figure 35*, it is possible to establish a threshold for the ratio above which the detected objects can be identified as pedestrians.

6.4 Doppler Principle for Human Identification

As mentioned before, when the transmitted signal reaches a moving object, the signal reflected from the object will have a Doppler shift that is proportional to the velocity of this object. For a rigid object the Doppler shift will be a constant value. A walking human is composed of body parts (arms, legs and torso) moving at different speeds and directions relative to each other. Thus, the Doppler signal from a human will be more complex. The movement of a human walking also can be described as a periodical with different periodicity according to the speed and it can be assumed that a reflected signal will contain this periodicity.

Using this principle, a CW radar system for detection and classification of humans based on their walking motion is presented in [31]. By analyzing the data using a short-time FFT, it is possible to obtain a Doppler signature that is very characteristic of humans.

A spectrogram of a human walking is shown in *Figure 36*. As can be seen the movement of the legs, arms and torso cause different components to the Doppler frequency. At some time-instances the movement of legs and arms causes a clearly detectable deviation from the signal of the torso (the spread in the frequency is large). However, in other time-instances the difference is very small (spread is small) and difficult to detect.

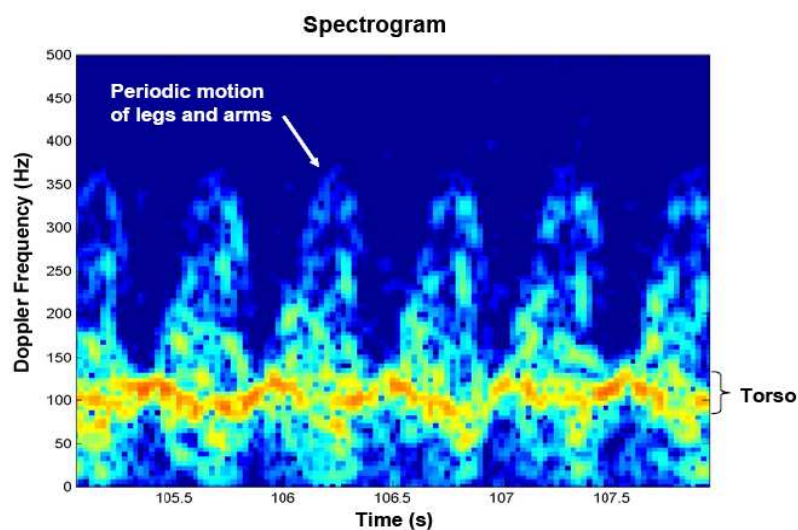


Figure 36. Spectrogram of a human walking obtained taking a succession of FFTs with a short time window using the output data of a CW radar at 10.525 GHz [34].

Also visible are the periodic changes of the frequency spread as a function of time. In order to identify a human by detecting these periodic changes the measurement system has to observe a human walking at least a couple of seconds. This may limit its use in applications requiring real time data.

6.5 Future Radar for Human Identification

At the beginning of this chapter, SAR systems are introduced since they are able to create an image of the observed area and have potential for high spatial resolution. However, the main problem of SAR is that it cannot make observations in all required directions (i.e., in front of the radar). This reason makes SAR an unsuitable solution.

Then, polarimetric radars are also introduced with unclear results. The differences between the signals reflected from a human in vertical and horizontal polarization are used to establish a criterion to identify humans. However, more measurements are needed in order to test if the polarization signal is usable as method for identification purposes in a complex environment.

The difference in the power of the signals reflected from a human at two different frequencies may provide enough information to set a criteria to identify human targets from non-human targets as is demonstrated in Section 6.3. This technique is able to detect and identify humans. Further research should be done to investigate which frequencies provide the most useful information about the target.

Finally, the effects of periodic movement of the different parts of a human (i.e., legs, arms, torso) on the reflected signal can also be used to identify humans as presented Section 6.4. However, one of the main problems found is that in order to obtain this periodicity, the radar needs at least a couple of seconds to identify a human, and this may be too slow for situation requiring real time data.

Chapter 7

Summary and Conclusion

The main objective of this thesis was to evaluate the capabilities and limitations of a commercial automotive radar for human detection applications in work machine environments. The results of this study show that the configuration of this LRR evaluated is not suitable for the intended application. In order to justify this claim, in this chapter a summary of each part of this thesis is presented and the final conclusions are drawn.

In the second chapter, it is demonstrated how the FMCW radar is able to obtain distance and speed information. Moreover, working at millimeter range allows reduction of the size of the antenna and consequently the whole system. On the negative side, however, heavy weather conditions create problems working at millimeter range. The attenuation caused by the atmosphere is high and the attenuation caused by rain increase with the frequency. In low range human detection application of around 30 m or less, nevertheless, this is not such a limiting factor.

In the third chapter, in order to investigate which alternative technologies are also possible, ultrasonic proximity sensors, laser scanners, infrared sensors and image processing are explained. Ultrasonic proximity sensors are a suitable solution in very short range human detection applications, such as 5 meters or less. Laser scanners could also offer a solution, however, they are not able to work under severe weather conditions. Similarly, image processing appears as another possible solution, as it is able to obtain real information about the environment. The algorithms to discriminate humans, however, require a high computational power.

In the fourth chapter, the automotive long range radar 77 GHz generation 2 is explained in depth. The most interesting finding is the configuration of the radar and the degradation of the range resolution in the receiver. In the fifth chapter, the measurements to determine the limitations of this radar in low range human detection applications are realized. As was expected, there are considerable differences between the limitations that the manufacturer provides with the limitations actually found in the measurements. The first measurements showed a considerable reduction in the maximum range, decreasing from 200 m down to 90 m. However, this degradation in range is not a limiting factor, as the range desired in this study is only 30 m. One unanticipated finding was that the range accuracy is even better than the specifications. The most interesting finding was the limited ability in range resolution: 3 m at distance of 15 m and 4 m at a distance of 30. This result is the main limitation of this radar. Another important finding was that the FOV has been reduced by 3° (from 16° to 13°).

The main reason affirming that this radar is not able to fulfil the requirements set in the research objective is the short range resolution. The radar is only able to distinguish a human from a large metal object or from a wall when the radial distance between both is larger than 3 m. Thus, in a human security application it is not possible to implement this radar in a complex environment with multiple targets present in the FOV, as in a dangerous situation this significant failing in range resolution could not help to avoid an accident. This result may be explained by the fact that when a human is close to another target with a larger RCS, the signal returned from the human has a close beat frequency and, furthermore, it has less power, and the radar determines it as the same target.

The LRR has a maximum bandwidth of 500 MHz which gives an ideal resolution of 0.3 m, however, the actual configuration only uses a bandwidth of 180 MHz which gives an ideal resolution of 0.8 m. Even though this ideal range resolution is a theoretical limitation, the actual configuration could be improved. As can be seen in Section 4.5, the range resolution can decrease in the receiver. Increasing the frequency resolution in the receiver will improve the ability of the radar to distinguish both targets, that is, to improve the quality of range resolution. For this, increasing the sampling rate in the ADC increases the number of samples in the frequency spectrum which will improve the frequency resolution. However, the period of the transmitted signal will increase in order to allow enough time to sample the beat frequency, which will reduce the update

rate. As can be observed, there is a compromise between the range resolution and update rate.

Another important limiting factor is the almost non-existent angular resolution, as when two humans at the same radial distance can only be detected as separate targets when they are at the edge of the FOV. In order to improve the angular resolution, more advanced algorithms in detection of arrival should be implemented in the radar.

As mentioned previously, this radar has been considered non-suitable for human detection applications in work machine environments, however, in flat open areas the radar presents a range up to 90 m with 13° of FOV. For this reason, these characteristics could be sufficient in other human detection applications.

As stated at the beginning of this thesis, there are two types of automotive radars, LRRs and SRRs. The measurements showed that with a LRR the maximum range that was specified as 200 m for car-type target was only 90 m for a human target. Since the SRRs operate on the same principles as the LRRs, similar reduction in detection range can also be expected for them.

The tested radar could only be used to detect human and other targets, not to identify which ones were humans and which ones were not. In Chapter 6, the possible radar technologies for human identification were discussed. The greatest potential this was found to be the combined use of two radars operating at different frequencies. Investigating this might be possible in the future by combining two automotive radars operating at two frequencies. However, instead of this LRR generation 2, the LRR generation 3 should be used since it will have a wider FOV (30°) and improvements in both range and angular resolution [34]. The production of this series will begin in 2009.

The other potential method for human identification is the Doppler technique. Using the periodicity in the reflected signal from a human is possible to recognize humans. This technique, however, may be too slow for this application.

References

- [1] ETSI Intelligent Transport, *Technical characteristics and test methods for radar equipment operating in the 76 GHz to 77 GHz band*, ETSI EN 301 091, 2006.
- [2] ETSI Intelligent Transport, *Short range radar equipment operating in the 24 GHz range*, ETSI EN 302 288-1, 2008.
- [3] IEEE Aerospace & Electronic Systems Society, *IEEE Standard Letter Designations for Radar-Frequency Bands*, IEEE Std 521-2002 Revision of IEEE Std 521-1984, 2002.
- [4] M. Skolnik, *Radar Handbook Third Edition*, Mc Graw Hill, 2008.
- [5] N. Yamada, *Radar Cross Section for Pedestrian in 76 GHz Band*, Toyota Central Research & Development Labs, 2004. http://www.tytlabs.co.jp/english/review/rev394epdf/e394_046yamada.pdf.
- [6] E. Smith, *Centimeter and millimeter wave attenuation and brightness temperature due to atmospheric oxygen and water vapour*, Radio Science, vol. 17, 1982.
- [7] J. Hernandez, J. Urena, J. Garcia, M. Mazo, D. Hernanz, J. Derutin and J. Serot, *Ultrasonic ranging sensor using simultaneous emissions from different transducers*, IEEE Transactions on Ultrasonics, Ferroelectrics and Frequency Control, pp. 1660 – 1670, Volume 51, Issue 12, Dec. 2004.
- [8] D. Noyce, R. Dharmaraju and J. Lehman, *An Evaluation of Technologies for Automated Detection and Classification of Pedestrians and Bicyclist*, Massachusetts Highway Department report, 2002. http://www.topslab.wisc.edu/publications/noyce_2001_0049.pdf.
- [9] Z. Yi, H. Khing, C. Seng, Z. Wei, *Multi-ultrasonic sensor fusion for mobile robots*, IEEE Int. Symposium on Intelligent Vehicles, pp.387-391, 2000.
- [10] D. Beckwith and K. Hunter, *Passive Pedestrian Detections at Un-Signalized Crossings*, 77th Annual Transportation Research Board Meeting, Paper No 980725, 1998.
- [11] O. Manolov, S. Noikov, P. Bison and G. Trainito, *Indoor Mobile Robot Control for Environment Information Gleaning*, IEEE Int. Symposium on Intelligent Vehicles, pp 602-607, 2000.
- [12] K. Song, C. Chen and C. Huang, *Design and Experimental Study of an Ultrasonic Sensor System for Lateral Collision Avoidance at Low Speeds*, IEEE Intelligent Vehicle Symposium, pp.647-652, 2004.

- [13] S.A. Johnston, E. N. Mazzae and W.R. Garrott, *An Evaluation of Electronic Pedestrian Detection Systems for School Buses*, SAE Paper 960518, 1996.
- [14] K. C. Fuerstenberg, K. Dietmayer and V. Willhoeft, *Pedestrian Recognition in Urban Traffic Using a Vehicle-based Multilayer Laserscanner*, IEEE Intelligent Vehicles Symposium, pp. 31-35, 2002.
- [15] K. Fuerstenberg and V. Willhoeft, *Pedestrian Recognition in Urban Traffic Using Laser Scanners*, 8th World Congress on Intelligent Transport Systems, paper 551, 2001.
- [16] H. Zhao and R. Shibasaki, *A Novel System for Tracking Pedestrians Using Multiple Single-row Laser Range Scanners*, IEEE Trans. On Systems, Man and Cybernetics, Vol. 35, No. 2, pp283-291, 2005.
- [17] K. Fuerstenberg and K. Dietmayer, *Object Tracking and Classification for Multiple Active Safety and Comfort Applications Using a Multilayer Laserscanner*, IEEE Intelligent Vehicle Symposium, pp. 802-807, 2004.
- [18] D. Streller and K. Dietmayer, *Multiple Hypothesis Classification with Laser Range Finders*, IEEE Intelligent Transportation Systems Conference, pp195-200, 2004.
- [19] K. C. Fuerstenberg and J. Scholz, *Reliable Pedestrian Protection Using Laser-Scanners*, IEEE Intelligent Vehicles Symposium, Las Vegas, June 2005.
- [20] J. Kerridge, A. Armitage, D. Binnie and L. Lei, *Monitoring the Movement of Pedestrians Using Low-Cost Infrared Detectors: Initial Findings*, Transportation Research Record No. 1878, pp. 11-18, 2004.
- [21] D.T. Linzmeier, D. Vogt, R. Prasanna, M. Mekhaieel, and K. C.J. Dietmayer, *Probabilistic Signal Interpretation Methods for a Thermopile Pedestrian Detection System*, IEEE Intelligent Vehicles Symposium, 2005.
- [22] D. Linzmeier, M. Mekhaieel, J. Dickman and K. Dietmayer, *Pedestrian Detection with Thermopiles Using an Occupancy Grid*, IEEE Intelligent Transportation Systems Conference, pp. 1063-1068, 2004.
- [23] E. Morimoto, M. Suguri, and M. Umeda. *Obstacle Avoidance System for Autonomous Transportation Vehicle based on Image Processing*, Agricultural Engineering International: the CIGR Journal of Scientific Research and Development, Manuscript PM 01 009. Vol. IV., December 2002.
- [24] T. Kalinke, C. Tzomakas, and W. von Seelen, *A Texture based Object Detection and an Adaptive Model-based Classification*, IEEE Intelligent Vehicles Symposium 98, pp. 341-346, Stuttgart, Germany, October 1998.
- [25] R. Hartley and A. Zisserman, *Multiple View Geometry in Computer Vision*, Cambridge, U.K., 2000.

- [26] Y. W. Xu, X. B. Cao and H. Qiao, *A Low-Cost Pedestrian Detection System with a Single Optical Camera*, Proceedings of the 6th World Congress on Intelligent Control and Automation, Dalian China, June 21-23 2006.
- [27] K. Strohm, R. Schneider and S. Wenger, *Kokon: A Joint Project for the Development of 79 GHz Automotive Radar Sensors*, IEEE Radar Symposium, 2005
- [28] S. Piper, *Homodyne FMCW Radar Range Resolution Effects with Sinusoidal Nonlinearities in the Frequency Sweep*, IEEE International Radar Conference, 1995.
- [29] F. Harris, *On the Use of Windows for Harmonic Analysis with the Discrete Fourier Transform*, Proceedings of the IWWW, vol. 66, no. 1, 1978.
- [30] A.G. Yarovoy, L.P. Ligthart, J. Matuzas and B. Levitas, *UWB Radar for Human Being Detection*, IEEE A&E Systems Magazine, May 2008. <http://www.ist-europcom.org/upload/documents/hbd.pdf>.
- [31] M. Otero, *Application of a continuous wave radar for human gait recognition*, Technical paper, The MITRE Corporation, 2005. http://www.mitre-corporation.com/work/tech_papers/tech_papers_05/05_0330/05_0330.pdf.
- [32] T. Nakane and K. Soshi, *A study on recognition of pedestrians using dual band radar*, ITS World Congress, Seoul, October, 1998.
- [33] T. Nakane and K. Soshi, *Animal body detecting system utilizing electromagnetic waves*, US Patent 6072173, 2000. <http://www.patentstorm.us/patents/6072173/description.html>.
- [34] Robert Bosch GmbH, Automotive Equipment, *Third-Generation long Range Radar, August 2008*. <http://www.bosch-presse.de/TBWebDB/en-US/Presstext.cfm?id=3693>.
- [35] Department of Physics & Astronomy, University of Hawaii, *RF Atmospheric Absorption/Ducting*. http://www.phys.hawaii.edu/~anita/web/paperwork/currently%20organizing/Military%20EW%20%20Handbook%20Excerpt/rf_absor.pdf.
- [36] Embedded Design India, *An Introduction to Adaptive Cruise Control (ACC)*, http://www.embeddeddesignindia.co.in/STATIC/PDF/200810/EDIOL_2008OCT23_DSP_TA_02.pdf?SOURCES=DOWNLOAD.
- [37] Cnes introduction to remotely sensed data, <http://ceos.cnes.fr:8100/cdrom-00b2/ceos1/irsd/figures/24.htm>.

Appendix

System Parameters of the LRR2

System Parameter	Value
Transmit frequency	76 - 77 GHz
Maximum transmit power	10 dBm
Number of beams	4
Polarization	45 deg Linear
Antenna gain	28 dBi
Azimuth field of view: Range	±8 deg
Accuracy	±0.1°-0.4°
Elevation field of view	±2 deg
Target detection distance: Range	2 - 200 m
Accuracy	±0.5 m
Resolution	2.0 m
Relative velocity: Range	-60 - +20 m/s
Accuracy	±0.25 m/s
Resolution	1.1 m/s
Number of ramps	3
Maximum frequency modulation sweep	500 MHz
Max. num. of detect. objects	32
Update rate	~10 Hz
Power consumption	13 W